



King Saud University  
**Arabian Journal of Chemistry**  
www.ksu.edu.sa  
www.sciencedirect.com



REVIEW

# Sulfated tin oxide (STO) – Structural properties and application in catalysis: A review



Ravi Varala<sup>a,c,\*</sup>, Venugopalarao Narayana<sup>b</sup>, Sripad R. Kulakarni<sup>c</sup>, Mujeeb Khan<sup>d</sup>, Abdulrahman Alwarthan<sup>d</sup>, Syed F. Adil<sup>d,\*</sup>

<sup>a</sup> Polymers Department, Institute de Fisica de Sao Carlos, University of Sao Paulo, Sao Carlos Campus, P.O. Box 369/13560-970, Brazil

<sup>b</sup> Neuland Pharma Research Lab, Bonthapalli, Hyderabad, Telangana, India

<sup>c</sup> Department of Chemistry, RGUKT-Basar, Mudhole, Adilabad 504107, Telangana, India

<sup>d</sup> Department of Chemistry, College of Science, King Saud University, P.O. 2455, Riyadh 11451, Saudi Arabia

Received 9 December 2015; accepted 26 February 2016

Available online 4 March 2016

**KEYWORDS**

Sulfated tin oxide;  
Catalysis;  
Reusability;  
Heterogeneous reactions;  
Biodiesel;  
Organic transformations

**Abstract** Catalysis is an important area of chemistry, with an extensive amount of work going on in this area of sciences, toward synthesis and evaluation of newer catalysts. There are many reports for different conversion reactions such as oxidation, reduction, coupling, alkylation, and acylation for which various catalysts have been used such as mixed metal oxides, metal nanoparticles, metal organic complexes and many others. Among the many catalysts reported, the one catalyst that caught our attention due to its exploitation for a plethora of organic conversions is the sulfated tin oxide (STO), which is due to the low cost, greater stability and high efficiency of the catalyst. In this review, we have attempted to compile data about the structural properties of STO, and its applications as catalysts in various organic synthesis are presented. The literature data up to 2014 were collected and considered for the review.

© 2016 The Authors. Production and hosting by Elsevier B.V. on behalf of King Saud University. This is an open access article under the CC BY-NC-ND license (<http://creativecommons.org/licenses/by-nc-nd/4.0/>).

**Contents**

|                                   |     |
|-----------------------------------|-----|
| 1. Introduction . . . . .         | 552 |
| 1.1. Acidity measurement. . . . . | 553 |
| 1.2. FT-IR spectroscopy . . . . . | 553 |

\* Corresponding authors. Tel.: +966 114670439 (S.F. Adil).

E-mail addresses: [ravivarala@ifsc.usp.br](mailto:ravivarala@ifsc.usp.br) (R. Varala), [sfadil@ksu.edu.sa](mailto:sfadil@ksu.edu.sa) (S.F. Adil).

Peer review under responsibility of King Saud University.



|         |   |     |
|---------|---|-----|
| 1.3.    | Effects on the STO catalysts due to sulfate content on its surface . . . . .  | 553 |
| 1.4.    | Thermal stability studies of tin oxide . . . . .  | 554 |
| 1.5.    | STO acidity: a solid-state NMR spectroscopy perspective . . . . .   | 555 |
| 1.6.    | Physicochemical characteristic of mixed metal oxide of sulfated Sn and rare earth metals . . . . .                                | 556 |
| 1.7.    | XRD analysis . . . . .  | 556 |
| 1.8.    | TPD studies of the STO catalysts . . . . .  | 556 |
| 1.9.    | Scanning Electron Microscopic (SEM) analysis . . . . .  | 557 |
| 2.      | Esterification and transesterification . . . . .  | 557 |
| 2.1.    | Free fatty acids (FFA) esterification . . . . .   | 557 |
| 2.2.    | Waste cooking oil transesterification . . . . .   | 557 |
| 2.3.    | Esterification of free fatty acids (FFAs) in crude palm oil . . . . .   | 557 |
| 2.4.    | Optimized preparation of <i>Moringa oleifera</i> methyl esters . . . . .  | 559 |
| 2.5.    | Transesterification reaction using biodiesel as co-solvent . . . . .  | 559 |
| 2.6.    | SnO <sub>2</sub> –SiO <sub>2</sub> : <i>Croton megalocarpus</i> oil for bio-diesel production . . . . .                           | 560 |
| 2.7.    | Biodiesel by catalytic reactive distillation powered by metal oxides . . . . .  | 560 |
| 2.8.    | Esterification and transesterification on Fe <sub>2</sub> O <sub>3</sub> -doped sulfated tin oxide catalysts . . . . .            | 560 |
| 2.9.    | Esterification and transesterification on Al <sub>2</sub> O <sub>3</sub> -doped sulfated tin oxide solid acid catalysts . . . . . | 560 |
| 2.10.   | Synthesis of sulfated silica-doped tin oxides and their high activities in transesterification . . . . .                          | 560 |
| 2.11.   | Application of sulfated tin oxide in transesterification and bio-diesel production . . . . .                                      | 560 |
| 2.11.1. | The heterogeneous transesterification of <i>Jatropha curcas</i> oil . . . . .   | 561 |
| 2.11.2. | Esterification of free fatty acids in crude palm oil . . . . .  | 561 |
| 2.11.3. | Synthesis of biodiesel <i>via</i> acid catalysis . . . . .  | 561 |
| 2.11.4. | Biodiesel fuel production in fixed bed reactor under atmospheric pressure . . . . .   | 561 |
| 2.11.5. | STO-Catalyzed esterification and etherification reactions . . . . .   | 561 |
| 3.      | Catalytic application of sulfated tin oxide in organic synthesis . . . . .  | 562 |
| 3.1.    | Synthesis of 7-hydroxy-4-methyl coumarin using Pechmann condensation method . . . . .   | 562 |
| 3.2.    | Baeyer–Villiger oxidation and acetalization of cyclic ketones . . . . .   | 562 |
| 3.3.    | Synthesis of 2,4,5-triaryl-1 <i>H</i> -imidazole derivatives . . . . .  | 562 |
| 3.4.    | Dehydration of xylose . . . . .   | 563 |
| 3.5.    | Friedel–Crafts acylation of toluene . . . . .   | 563 |
| 3.6.    | Deprotection of silyl ether . . . . .   | 564 |
| 3.7.    | Synthesis of 2,4-diphenyl-4,6,7,8-tetrahydrochromen-5-one . . . . .   | 564 |
| 3.8.    | C3-alkylation and <i>O</i> -alkylation of 4-hydroxycoumarins . . . . .  | 564 |
| 3.9.    | Efficient one-pot synthesis of 7,8-dihydro-2 <i>H</i> -chromen-5-ones . . . . .   | 564 |
| 3.10.   | Facile transesterification of ketoesters . . . . .  | 565 |
| 3.11.   | Aldol condensation and benzylation . . . . .  | 566 |
| 3.12.   | Synthesis of structurally diverse β-acetamido ketones and aryl-14 <i>H</i> -dibenzo(a,j) xanthenes . . . . .                      | 566 |
| 3.13.   | Selective dehydration of sorbitol . . . . .   | 566 |
| 3.14.   | One-pot synthesis of naphthopyranopyrimidines . . . . .   | 567 |
| 3.15.   | Synthesis of pyrimidopyrimidines . . . . .  | 567 |
| 3.16.   | Catalytic pyrolysis of cellulose: synthesis of light furan compounds . . . . .  | 568 |
| 3.17.   | Mesostructured sulfated tin oxide and its high catalytic activity in esterification and Friedel–Crafts acylation . . . . .        | 568 |
| 3.18.   | Alkylation of phenol with methanol . . . . .  | 568 |
| 3.19.   | Selective nitration of phenol . . . . .   | 569 |
| 3.20.   | Alkylation of hydroquinone with <i>tert</i> -butanol . . . . .  | 569 |
| 3.21.   | Direct oxidation of <i>n</i> -heptane to ester over modified sulfated SnO <sub>2</sub> catalysts under mild conditions . . . . .  | 569 |
| 3.22.   | Dealkylation of anisole to phenol using lanthanum-sulfated SnO <sub>2</sub> . . . . .   | 570 |
| 3.23.   | Olefin polymerization and hydrogenation catalysis . . . . .   | 570 |
| 3.24.   | Synthesis and hydrolysis of dimethyl acetals . . . . .  | 571 |
| 3.25.   | Ethanol oxidation . . . . .   | 571 |
| 3.26.   | Catalysis in direct coal liquefaction . . . . .   | 571 |
| 4.      | Conclusion . . . . .  | 571 |
|         | Acknowledgments . . . . .   | 571 |
|         | References . . . . .  | 572 |

## 1. Introduction

Due to their excellent physicochemical and fascinating surface properties, metal oxides represent the important class of materials which have profound implications in the field of catalysis (Ren et al., 2012). These materials have been widely applied as solid catalysts, either as active phases or as support materials (Gawande et al., 2012). So far, various metal oxides have been extensively exploited as industrial catalysts for several commercially important reactions (Arena et al., 2015). Metal oxide catalyst is either used in its pure form, or in many cases is supported on other oxides, where the catalytic activity is enhanced by the interaction between two oxides (Park et al., 2015). Particularly, in the field of heterogeneous catalysis, metal oxides have been extensively applied for several important organic transformations, due to their excellent acid–base and redox properties (C  lerier and Richard, 2015). Among different metal oxides, tin oxide ( $\text{SnO}_2$ ) has attracted immense interest of the scientific community, due to its dual valency and its ability to attain more than one oxidation state (Batzell and Diebold, 2005). Usually,  $\text{SnO}_2$  prefers to possess the oxidation states of  $2+$  or  $4+$ , which greatly promotes the variation in the composition of surface oxygen, and thus, the  $\text{SnO}_2$  exhibits varied surface properties, which has a significant importance in catalysis. Furthermore, due to the excellent acidic, basic, oxidizing and reducing surface properties,  $\text{SnO}_2$  acts as an active heterogeneous catalyst for many important organic reactions. From the earlier observations, it has been proved that the efficiency of a heterogeneous catalyst depends on the intrinsic catalytic activity of its component in addition to its texture and stability. The mineral form of  $\text{SnO}_2$  is called ‘cassiterite’ (Fig. 1), and it is the main ore of tin (Greenwood and Earnshaw, 1984). In tin chemistry,  $\text{SnO}_2$  is the most vital raw material. This is colorless solid that is diamagnetic and amphoteric in nature.

It has been reportedly used as catalyst in addition to the vanadium oxide for the synthesis of carboxylic acids and acid anhydrides by oxidation of aromatic compounds. It is being utilized in various ways as an opacifier and white colorant in ceramic glazes (Searle, 2008), as a polishing powder (Jensen, 2002) in glass coating and in gas sensing (Watson, 1984).

The correct choice of the additives is very prominent in fine tuning the surface properties of a catalyst. Attempts were made as a mean to improve the tin oxide catalyst by adsorbing various anions such as sulfate or phosphate anions onto the tin oxide. The increase in the surface acidity of the modified oxide leads to the raise in activity of the catalyst. A strong acidity generated with the modification of metal oxides with sulfate anion is even stronger than 100% sulfuric acid and thus acts as super acid catalysts for several commercially important reactions. Acid catalysis has a vital industrial application, which is widely employed in the various isomerization, alkylation and cracking reactions that are used to upgrade oil and hence plays a crucial and important role in the petroleum industry. Large scale polymerization processes involve acids as catalysts and display activity for interconversion of ethanol and ethylene (hydration/dehydration reactions).

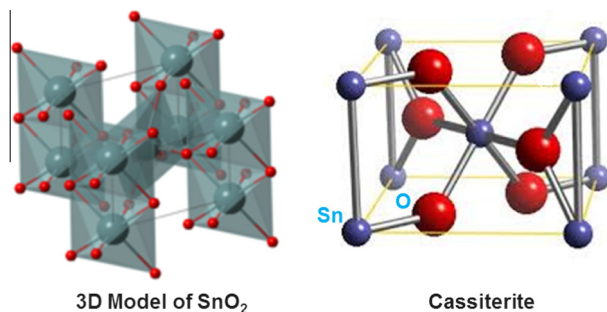


Figure 1 Tin oxide.

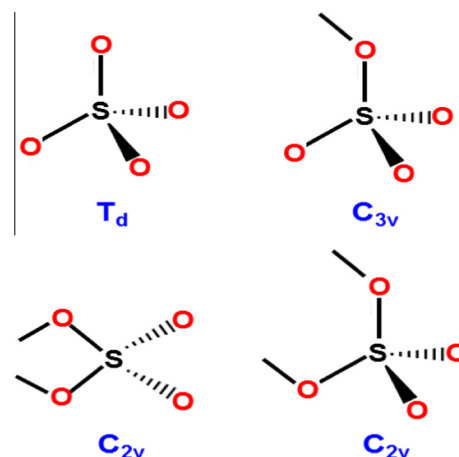


Figure 2 Different  $\text{SO}_4^{2-}$  symmetries (Brown And Hargreaves, 1999).

Table 1 Solid super acids and their acidic strength (Arata et al., 2003).

| Catalyst                            | Calcination temperature ( $^{\circ}\text{C}$ ) | Highest acid strength <sup>a</sup> ( $H_0$ value) |
|-------------------------------------|--|---|
| $\text{SO}_4/\text{SnO}_2$          | 550  | −18.0   |
| $\text{SO}_4/\text{ZrO}_2$          | 650  | −16.1   |
| $\text{SO}_4/\text{HfO}_2$          | 700  | −16.0   |
| $\text{SO}_4/\text{TiO}_2$          | 525  | −14.6   |
| $\text{SO}_4/\text{Al}_2\text{O}_3$ | 650  | −14.6   |
| $\text{SO}_4/\text{Fe}_2\text{O}_3$ | 500  | −13.0   |
| $\text{SO}_4/\text{SiO}_2$          | 400  | −12.2   |
| $\text{WO}_3/\text{ZrO}_2^a$        | 800  | −14.6   |
| $\text{MoO}_3/\text{ZrO}_2$         | 800  | −13.3   |
| $\text{WO}_3/\text{SnO}_2$          | 1000   | −13.3   |
| $\text{WO}_3/\text{TiO}_2$          | 700  | −13.1   |
| $\text{WO}_3/\text{Fe}_2\text{O}_3$ | 700  | −12.5   |
| $\text{B}_2\text{O}_3/\text{ZrO}_2$ | 650  | −12.5   |

<sup>a</sup> Acid strengths were estimated by color change of Hammett indicator, TPD of pyridine, TPR of furan, and catalytic activity for various reactions.

Although with limited lifetimes, these sulfated metal oxides possess excellent ability to catalyze isomerization reactions, i.e. conversion of straight chain alkanes to more highly branched isomers, at low temperatures, which is a characteristic of very strong acid catalysts. Arata and his group has exploited a range of active sulfated oxides including those based on  $\text{SO}_4^{2-}/\text{ZrO}_2$ ,  $\text{SO}_4^{2-}/\text{SnO}_2$ ,  $\text{SO}_4^{2-}/\text{Fe}_2\text{O}_3$ ,  $\text{SO}_4^{2-}/\text{SiO}_2$ ,  $\text{SO}_4^{2-}/\text{TiO}_2$ ,  $\text{SO}_4^{2-}/\text{HfO}_2$  and  $\text{SO}_4^{2-}/\text{Al}_2\text{O}_3$  (Arata, 1990, 1996, 2009). It was reported that in order to obtain a catalyst with high activity, the sulfation must be performed on the amorphous precursors of the hydroxides or oxyhydroxides, however this was not found true for alumina ( $\text{Al}_2\text{O}_3$ ). Among various sulfation reagents available, either dilute sulfuric acid or an aqueous solution of ammonium sulfate has been commonly used by researchers. Sulfate, an additive among many has been detected to favor the formation of the tetragonal phase, while monoclinic form is one that is commonly found (Norman et al., 1994).

A number of diverse proposals have been made to explain the nature of the active catalytic site, mostly based across the symmetry of the coordinated sulfate ion (Brown and Hargreaves, 1999). However, a number of symmetries for  $\text{SO}_4^{2-}$  are possible in principle as depicted in Fig. 2. They can be distinguished by examination of the sample  $\text{S}=\text{O}$  stretching region ( $1200\text{--}900\text{ cm}^{-1}$ ) in the infrared spectra (Nakamoto, 1986). Both  $\text{C}_{2v}$  and  $\text{C}_{3v}$  forms have been in general exploited in the literature.

The sulfated tin(IV) oxide is one of the promising candidates for exhibiting the strongest acidity on the surface. The acid strength of sulfated tin oxide is proved to be higher than that of sulfated zirconia (Table 1, entries 1–2).

### 1.1. Acidity measurement

See Table 1.

The literature is abundant with reports wherein researchers have attempted characterization and employing the STO for various chemical transformations. A few characterization techniques are compiled below.

### 1.2. FT-IR spectroscopy

The IR spectra of sulfated tin(IV) oxide ( $x$ STO) in comparison with pure tin(IV) oxide (TO) are shown in Fig. 3 (Clearfield et al., 1994; Jogalekar et al., 1998; Mekhemer et al., 2005; Mekhemer, 2006). The appearance of the bands at 1382, 1190, 1155 and 1079  $\text{cm}^{-1}$  confirmed the presence of sulfate group.

The above observed features are in general attributed to triply bridging sulfate and bridged bidentate sulfate, as represented in Fig. 4.

Dabbawala et al. prepared the STO and studied the effect taken place due to calcination temperature using FT-IR. The spectra of the sulfated tin oxide catalysts are shown in Fig. 5. The bands/peaks at 1165, 1038, and 975  $\text{cm}^{-1}$  in the spectrum clearly indicate the presence of sulfated group and a bidentate chelation mode between the sulfate and tin. By the existence of the sulfate groups on the catalyst surface, a strong acidic nature can be realized.

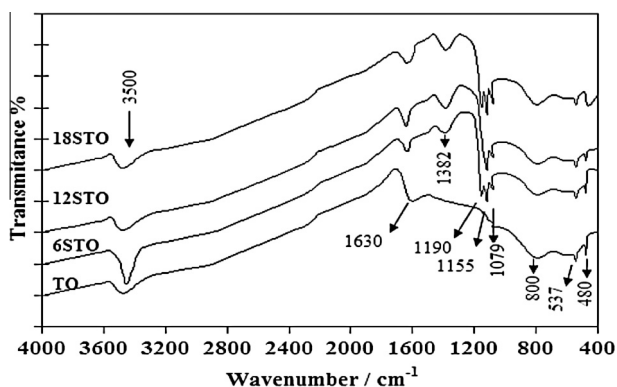


**Figure 3** FTIR spectra for  $x$ STO in comparison with TO catalysts (Khalaf et al., 2011).

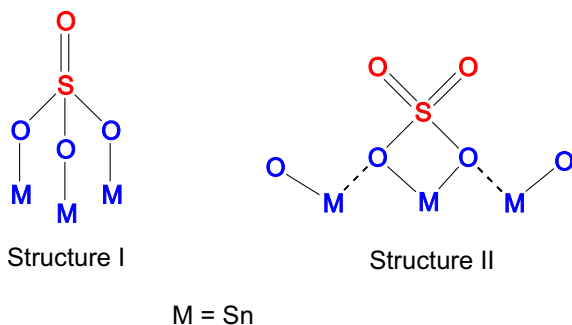


**Figure 4** Triply bridging sulfate (I) and bridged bidentate sulfate (II) (Khalaf et al., 2011).

The acidity of solids used as catalysts or catalyst carriers has been the subject of various investigations and reviews for a long time (Sheldon, 2000; José da Silva and Lemos Cardoso, 2013). It was learned by interaction with the active components (support effect) or by providing acidic sites which may make the acid catalyst bifunctional, thus influencing the properties of a catalyst.

The acid sites on metal oxides are believed to be due to the surface hydroxyl groups or a charge imbalance localized on the surface. The deficient amounts of localized electrons result from a local imbalance between positive and negative charges of the constituents and act as a Lewis acid for catalytic reactions. By substituting the metal ion with other metal ions possessing different charges a charge imbalance can be expected and new acid sites could be generated on the surface of doped and or mixed metal oxides (Connell and Dumesic, 1986; Hudlicky et al., 1999).

It is reported that some sulfated metal oxides produce super acid materials with surface acidity and much larger surface areas compared with those metal oxides without sulfate (Sheldon, 1993). In general, the reactions catalyzed by strong acids, many of these super acid compounds are found to be very good catalysts, and it is mainly because of the features such as acidity and surface area. With enlarged acid surface properties that come from the sulfation process as well as the existence of two metals that are able to absorb  $\text{H}_2$  and henceforth, the new system can be considered as a bifunctional catalyst. Sulfation enhances the strength of the weakest Lewis acid sites but poisons the strongest. In the case of highly loaded samples it also creates Bronsted acidity (Waqif et al., 1992).

### 1.3. Effects on the STO catalysts due to sulfate content on its surface

Khder and coworkers assessed the effect of calcination temperature and sulfate content on the acidity, structure and catalytic activity of sulfated tin oxides. Numerous catalysts were synthesized with different sulfate contents using different thermal treatment temperatures as shown in Table 2. An increase in  $\text{SO}_4^{2-}$  ions load resulted in consequent increase in  $\text{SnO}_2$  surface area irrespective of the calcinations temperature. It was observed that decrease in the surface area of both catalysts  $\text{SO}_4^{2-}/\text{SnO}_2$  and  $\text{SnO}_2$  resulted in increase in the calcination temperature. Based on these observations, the authors suggested that the presence of sulfate ions on the surface of tin oxide prevents a higher reduction in surface area provoked by an increase in the calcinations temperature, while Table 3 demonstrates the notable effect observed by both increase in the calcination temperature and increase in the sulfate content (Khder et al., 2008).

Khder and coworkers observed that when the catalyst contained the highest NAS and the highest amount of sulfate ions, the highest

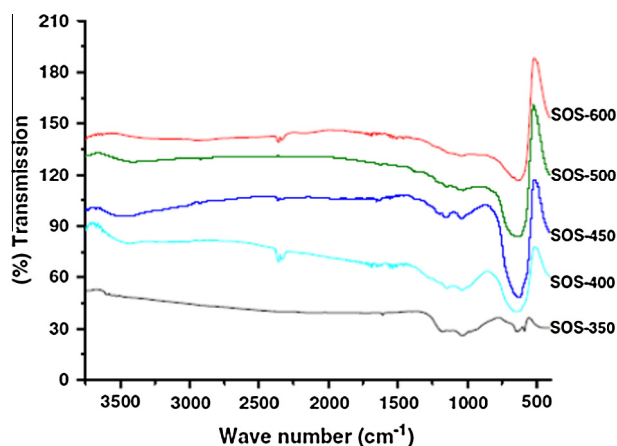


**Figure 5** FT-IR spectra of STO calcined at different temperatures (Dabbawala et al., 2013).

**Table 2** BET surface area measurements obtained from  $\text{SO}_4^{2-}/\text{SnO}_2$  catalysts synthesized at temperature of 400, 550, 750 °C (Khder et al., 2008).

| $\text{SO}_4^{2-}$ content on $\text{SnO}_2$ catalyst (wt%) | Surface area ( $\text{m}^2/\text{g}$ ) |        |        |
|---|--|--------|--------|
|   | 400 °C                                 | 550 °C | 750 °C |
| 0   | 61.2                                   | 46.3   | 20.4   |
| 1   | 69.9                                   | 52.3   | 28.5   |
| 5   | 76.2                                   | 64.7   | 36.5   |
| 15  | 90.2                                   | 80.8   | 57.2   |
| 20  | 101.3                                  | 87.3   | 62.5   |
| 30  | 129.5                                  | 100.8  | 70.1   |

conversions occurred in the acetic acid esterification with amyl alcohol and reusability studies of the catalyst were also studied. The graphical representation of conversion results reported is given in Fig. 6 (A), while Fig. 6(B) gives the results obtained from the reusability study of the catalyst. Based on this study, Khder and coworkers proposed that the presence of a covalent S=O bond may lead to the generation of strong Lewis acidity of the sulfate species, which act as electron withdrawing species, which is followed by the inductive effect, thereby making the Lewis acid strength of  $\text{Sn}^{+4}$  stronger as demonstrated by arrows in Fig. 7. On addition, the Lewis acid sites are converted to Bronsted acid sites in the presence of water, via proton transfer (Khder et al., 2008).

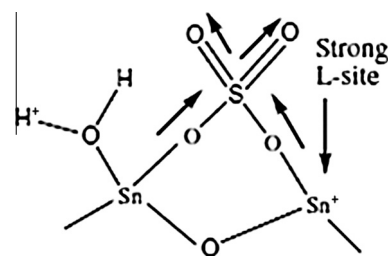


**Figure 7** A surface structure of sulfated tin oxide (Khder et al., 2008).

#### 1.4. Thermal stability studies of tin oxide

In order to study the surface properties, active sites and its strength, preparation of the sulfated tin oxide catalyst, has been carried out under different conditions and along with addition of other metal oxides by various research groups.

Khalaf reportedly studied the thermal stability of sulfated tin oxide (STO) and compared it with the tin gel. It was reported that the TG profile was found to be different with STO displaying three step mass loss while the precursor, unsulfated tin gel ( $\text{SnO}_2 \cdot x\text{H}_2\text{O}$ ) undergoes thermal degradation in two step mass loss. The precursor tin gel ( $\text{SnO}_2 \cdot x\text{H}_2\text{O}$ ) and STO show a mass loss of  $\sim 19.9\%$ , when heated up to 1273 K. The thermogram obtained is given in Fig. 8 (Khalaf et al., 2011).

**Table 3** Acidic properties of the  $\text{SO}_4^{2-}/\text{SnO}_2$  catalysts synthesized at temperatures of 400, 550, 750 °C (Khder et al., 2008).

| Calcination temperature (°C) | 400   |                             | 550        |                             | 750        |                             | Pyridine loss (wt%) | $t$ (°C) |            |
|------------------------------|---|-----------------------------|------------|-----------------------------|------------|-----------------------------|---------------------|----------|------------|
|                              | $\text{SO}_4^{2-}$ content on $\text{SnO}_2$ catalyst (wt%) | NAS ( $\text{meq g}^{-1}$ ) | $E_i$ (mV) | NAS ( $\text{meq g}^{-1}$ ) | $E_i$ (mV) | NAS ( $\text{meq g}^{-1}$ ) |                     |          | $E_i$ (mV) |
| 0                            | 0.20  | 0.20                        | -84        | 0.35                        | +27        | 0.14                        | -127                | 0.210    | 424.5      |
| 1                            | 0.31  | 0.31                        | -70        | 0.51                        | +194       | 0.24                        | -109                | 0.448    | 460.8      |
| 5                            | 0.38  | 0.38                        | -61        | 0.66                        | +316       | 0.30                        | -97                 | 0.667    | 468.4      |
| 15                           | 0.50  | 0.50                        | -27        | 0.83                        | +479       | 0.42                        | -54                 | 1.430    | 479.4      |
| 20                           | 0.56  | 0.56                        | +9         | 0.97                        | +510       | 0.51                        | -41                 | 1.841    | 482.0      |
| 30                           | 0.68  | 0.68                        | +25        | 1.30                        | +555       | 0.60                        | -23                 | 2.440    | 482.5      |

NAS: acid sites number;  $E_i$ : initial electrode potential indicates the maximum acid strength of the sites;  $t$ : pyridine loss temperature.

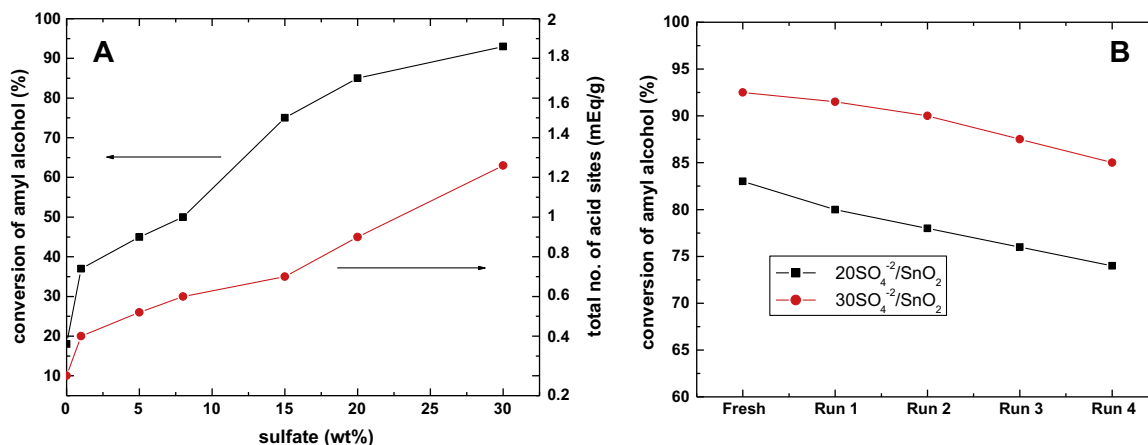


**Figure 6** (A) Relation between sulfate content, esterification reaction of acetic acid with amyl alcohol at 250 °C and surface activity. (B) Effect of reusability of catalysts at 250 °C amyl alcohol/acetic acid molar ratio 2:1 (Khder et al., 2008).

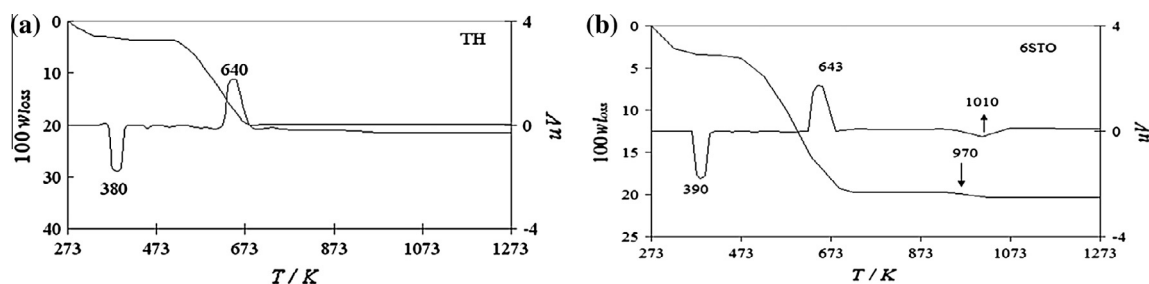


**Figure 8** TGA and DTA profiles for (a) tin(IV) gel (TH), and (b) sulfated tin(IV) oxide (6STO),  $w_{\text{loss}}$  is the mass fraction (Khalaf et al., 2011).

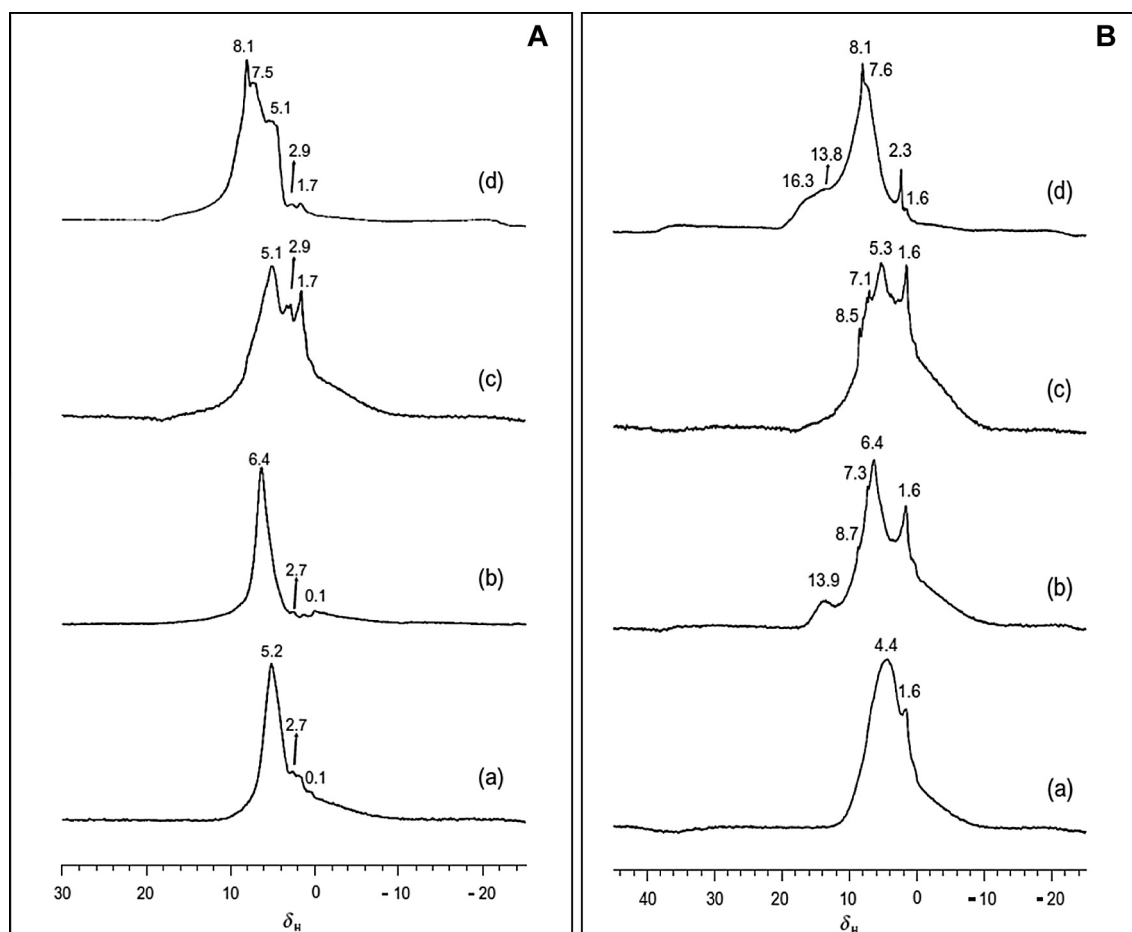


**Figure 9** (A)  $^1\text{H}$  MAS NMR spectra of ZrO<sub>2</sub> (a), SO<sub>4</sub><sup>2-</sup>/ZrO<sub>2</sub> (b), SnO<sub>2</sub> (c) and SO<sub>4</sub><sup>2-</sup>/SnO<sub>2</sub> (d). (B)  $^1\text{H}$  MAS NMR spectra of pyridine-*d*<sub>5</sub> loaded on ZrO<sub>2</sub> (a), SO<sub>4</sub><sup>2-</sup>/ZrO<sub>2</sub> (b), SnO<sub>2</sub> (c) and SO<sub>4</sub><sup>2-</sup>/SnO<sub>2</sub> (d) (Yu et al., 2009).

### 1.5. STO acidity: a solid-state NMR spectroscopy perspective

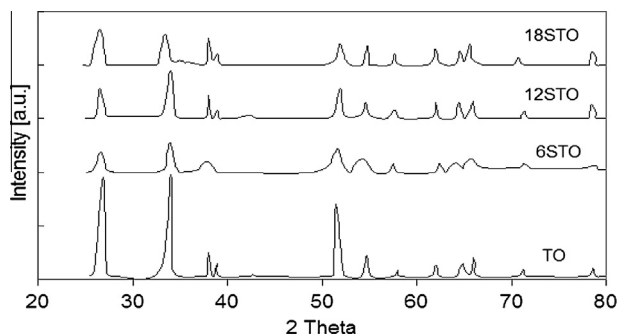
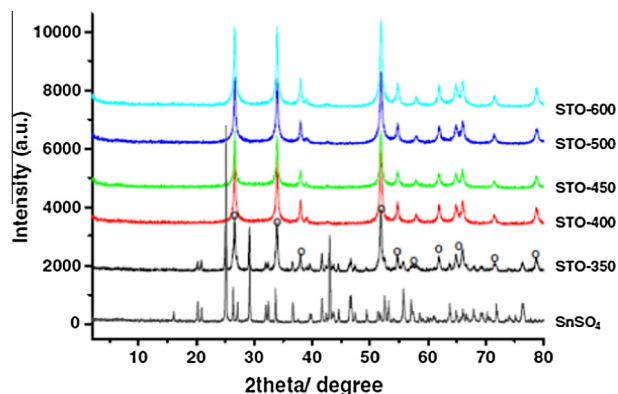
Yu et al. studied the acidic properties of SnO<sub>2</sub>, SO<sub>4</sub><sup>2-</sup>/SnO<sub>2</sub>, ZrO<sub>2</sub> and SO<sub>4</sub><sup>2-</sup>/ZrO<sub>2</sub>, by using solid-state NMR spectroscopy (Figs. 9 (A) and (B)). It was shown that new acidic sites were created when SO<sub>4</sub><sup>2-</sup> was able to interact with the hydroxyl groups of SnO<sub>2</sub> and ZrO<sub>2</sub>.  $^1\text{H}$ ,  $^{13}\text{C}$ , and  $^{31}\text{P}$  MAS NMR spectra of the above mentioned molecules showed that only on SO<sub>4</sub><sup>2-</sup>/SnO<sub>2</sub> a Bronsted acid site was

present. The acid strength of SO<sub>4</sub><sup>2-</sup>/ZrO<sub>2</sub> was weaker than that of SO<sub>4</sub><sup>2-</sup>/SnO<sub>2</sub> (Yu et al., 2009). Table 4 shows characterized and the textual properties of the prepared samples.

The authors compared the  $^1\text{H}$  NMR spectra obtained from the sulfated metal oxides and the corresponding metal oxides. It was found that the peaks with the larger chemical shifts were observed in case of sulfated metal oxides. It clearly proves that when the metal oxides were treated with sulfuric acid, the new acid sites were formed.

**Table 4** Textural properties of various samples (Yu et al., 2009).

| Samples   | $S_{\text{BET}}$<br>( $\text{m}^2 \text{g}^{-1}$ ) | Average crystal<br>size (nm) | Sulfate content<br>(wt%) | Color  |
|---|--|------------------------------|--------------------------|--------|
| ZrO <sub>2</sub>                                | 112  | 15.6                         | –                        | White  |
| SO <sub>4</sub> <sup>2-</sup> /ZrO <sub>2</sub> | 134  | 12.2                         | 2.30                     | White  |
| SnO <sub>2</sub>                                | 28   | 16.0                         | –                        | Yellow |
| SO <sub>4</sub> <sup>2-</sup> /SnO <sub>2</sub> | 93   | 4.8                          | 3.31                     | Yellow |

**Figure 10** X-ray powder diffractograms for  $x\text{STO}$  ( $x$  = different loading levels) in comparison with TO catalyst (Khalaf et al., 2011).**Figure 11** XRD patterns of STO calcined at different temperatures (O—SnO<sub>2</sub>) (Dabbawala et al., 2013).

### 1.6. Physicochemical characteristic of mixed metal oxide of sulfated Sn and rare earth metals

Binary mixed oxides of tin with three rare earth elements viz. La, Ce and Sm were reported by Jyothi et al. The co-precipitation method and sulfate treatment were employed, which was executed by treating the mixed hydroxides with sulfuric acid or ammonium sulfate (Jyothi et al., 2000a,b,c). The strength as well as the distribution of acid sites depends on both the preparation method and the mixed metal oxide composition. In the oxidative dehydrogenation of cyclohexanol and cyclohexane, the rare earth modified sulfated tin oxide catalysts proved to be more active when compared to the corresponding mixed oxide systems and sulfated tin oxide. The cerium promoted catalysts showed excellent selectivity toward dehydrogenation products, among the various sulfated oxide systems studied.

### 1.7. XRD analysis

XRD analysis is a famous technique for the analysis of crystalline nature of the metal salts and various phase changes that take place in the metal salt upon change in physiological conditions.

Numerous tin(IV) oxide catalysts, pure and surface-doped with different loading levels of sulfate, have been synthesized and characterized by Khalaf et al. using different characterization techniques (Khalaf et al., 2011). It is revealed from the structural investigation of the catalysts that the tin(IV) gel has the formula SnO<sub>2</sub>·2H<sub>2</sub>O. The addition of sulfate will not affect the crystalline structure of tin(IV) oxide (tetragonal phase) but it decreases the crystallite size and as a result increases the specific surface area.

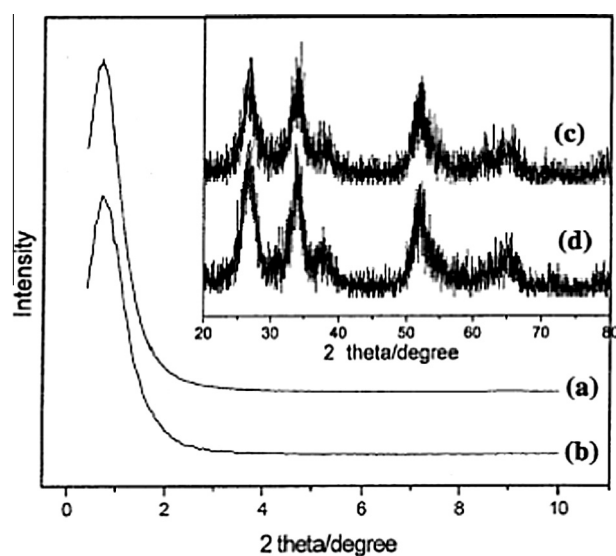
The sulfated samples, with different loading levels of sulfate by weight (6STO, 12STO and 18STO), XRD diffractograms obtained at calcination temperature 873 K are shown in Fig. 10. It is evident that all patterns are characteristic of pure SnO<sub>2</sub> phase with tetragonal rutile structure at  $2\theta = 26.54, 33.82$  and  $51.74$  (Khalaf et al., 2011).

Similar studies were carried out by Dabbawala and coworkers, wherein they prepared the STO and studied the phase transitions that take place due to calcination temperature using XRD, and the obtained XRD spectrum is given in Fig. 11. It is reported that the decomposition of SnSO<sub>4</sub> to SO<sub>4</sub><sup>2-</sup>/SnO<sub>2</sub> took place at a calcination temperature of 350 °C. For all the samples prepared, above the calcination temperature of 350 °C, a disappearance of characteristic diffraction peaks of SnSO<sub>4</sub> indicates the complete conversion to SO<sub>4</sub><sup>2-</sup>/SnO<sub>2</sub>.

Du et al. prepared a mesostructured sulfated tin oxide catalyst (MST) possessing large surface area (172 m<sup>2</sup>/g) while employing block copolymer as template, followed by the sulfation of the sample. They employed X-ray diffraction (XRD), transmission electron microscopy (TEM), thermogravimetric analysis (TG), and nitrogen adsorption methods to characterize the MST catalysts. The XRD analysis yielded spectrum with peaks at  $2\theta \sim 27, 34, 38, 52, 65$  as given in Fig. 12, which revealed that the samples possess tetragonal phase of crystalline SnO<sub>2</sub> (Du et al., 2006).

### 1.8. TPD studies of the STO catalysts

Furuta and coworkers measured the sulfated oxides acidity employing pyridine adsorption and ammonia adsorption and temperature-programmed desorption (TPD) studies. The two pyridine adsorption

**Figure 12** Small-angle XRD patterns of MST-500 (a) and MST-550 (b); and wide-angle XRD patterns of MS-500 (c) and MST-550 (d) (Du et al., 2006).

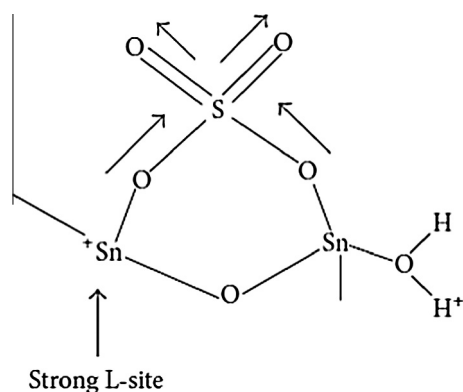


**Figure 13** Electron withdrawing effect of sulfate group on sulfated tin oxide.

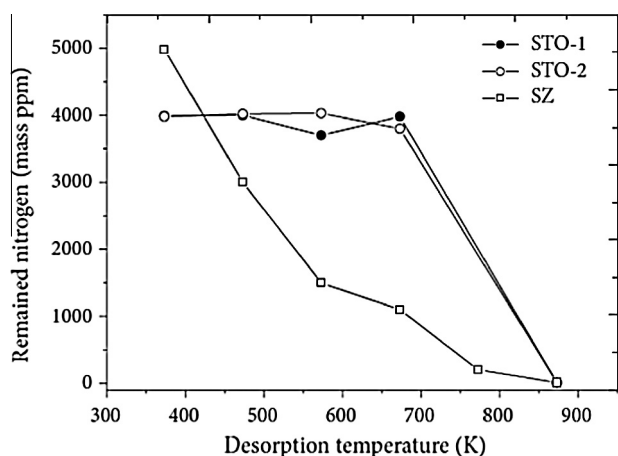


**Figure 14** Ammonia-TPD profiles of STO-1, STO-2, and SZ (sulfated zirconia) catalysts (Furuta et al., 2004a,b).

characteristic bands measured *via* FT-IR (i.e., 1445 and 1541  $\text{cm}^{-1}$ , resp.) confirms the presence of Lewis and Bronsted acids sites. It was observed that the band correspondent to Lewis acid sites had higher intensity in the compounds with a higher amount of  $\text{SO}_4^{2-}$  ions, and it is due to electron withdrawing effect of sulfate group, which thus increases the Lewis acidity of the Sn cations (Fig. 13).

By means of TPD technique, Fig. 14 shows the nitrogen content that remained on the catalyst surface, which was determined by elementary analysis of nitrogen. It clearly indicates that over a wide range of temperature, the tin catalysts possess a much higher acidity (Furuta et al., 2004a,b).

### 1.9. Scanning Electron Microscopic (SEM) analysis

Dabbawala and coworkers subjected the prepared STO samples to SEM-EDX studies to understand the morphology and elemental analysis. The presence of sulfur, tin and oxygen was observed from the SEM-EDX spectrum as seen in Fig. 15. It was also observed that the STO has a cubic morphology of the size 30–35 nm (Dabbawala et al., 2013).

## 2. Esterification and transesterification

Esterification reaction is an important reaction industrially as it is employed for the production of important chemicals, such as polyesters, biodiesel and glycerol, which is extensively used

in pharmaceutical formulations and food industries; hence, research toward finding a right catalyst has been extensively studied and sulfated tin oxide catalyst has been reported for various such reactions mentioned below.

### 2.1. Free fatty acids (FFA) esterification

Moreno et al. synthesized sulfated tin oxides with different sulfate contents from the hydroxylated tin oxide using precipitation method. They proved that upon sulfation, the  $\text{SnO}_2$  crystal growth could be inhibited. The  $\text{SO}_4^{2-}$  species strongly binds to the  $\text{SnO}_2$  surface and thus stabilizing its crystalline size against sintering (Moreno et al., 2011). The esterification of oleic acid increased with the increase in the surface acidity and a maximum conversion was achieved at 0.3 wt% sulfate content and 773 K calcination temperature. The reaction of  $\text{SnCl}_2 \cdot 2\text{H}_2\text{O}$  with  $\text{NH}_4\text{OH}$  resulted in the precipitation of  $\text{Sn}(\text{OH})_2 \cdot \text{H}_2\text{O}$  which on filtration, and the solid impregnation with  $\text{H}_2\text{SO}_4$ , followed by thermal treatment leads to the synthesis of  $\text{SO}_4^{2-}/\text{SnO}_2$  solid catalyst. It was observed from the thermogravimetric data that the surface area of the catalyst was reduced at higher temperatures. Moreno and group formulated an important factor of the relationship between the solid catalyst activity and the acidity using Hammett Indicators. This relation can be easily understood in the esterification reaction of oleic acid with ethyl alcohol as illustrated in Fig. 16. The catalyst with the highest NAS was more active; however, it does not have the highest surface area; this fact further supports that in the acid solid-catalyzed esterification reactions, the acid sites are also essential. The BET surface area data and thermogravimetric analysis of the prepared catalyst were concluded in Table 5.

### 2.2. Waste cooking oil transesterification

Lam and co-workers synthesized a superacid sulfated tin oxide catalyst by employing the impregnation method (倉員貴昭, 2011). To increase the catalytic activity of  $\text{SnO}_2$ , it was mixed with  $\text{SiO}_2$  and  $\text{Al}_2\text{O}_3$  respectively at different weight ratios and the bimetallic effect was probed.

The transesterification reaction temperature (100–200 °C) on the yield of FAME using different bimetallic catalysts was studied at different weight ratios (Fig. 17). It was observed that increasing the temperature from 100 to 150 °C, authors noted tremendous increase in the yield of FAME for all types of catalyst tested.

### 2.3. Esterification of free fatty acids (FFAs) in crude palm oil

Nuithitikul et al. studied the activities of sulfated iron–tin mixed oxide catalysts, which were prepared using co-precipitation method, for esterification of free fatty acids in crude palm oil (Nuithitikul et al., 2011). The varied parameters for the synthesis were iron precursor, sulfate concentration and calcination temperature. Iron sulfate was found to be the best precursor from the observations made. With the increase in sulfate content, the activity of the catalyst was found to increase. In reuse of the catalyst, its stability was improved by the addition of the iron oxide to the sulfated tin oxide. The optimum calcination temperature was 450 °C. Hence, sulfated iron–tin oxide was found to be the best catalyst for the esterification of fatty acids in comparison with STO.

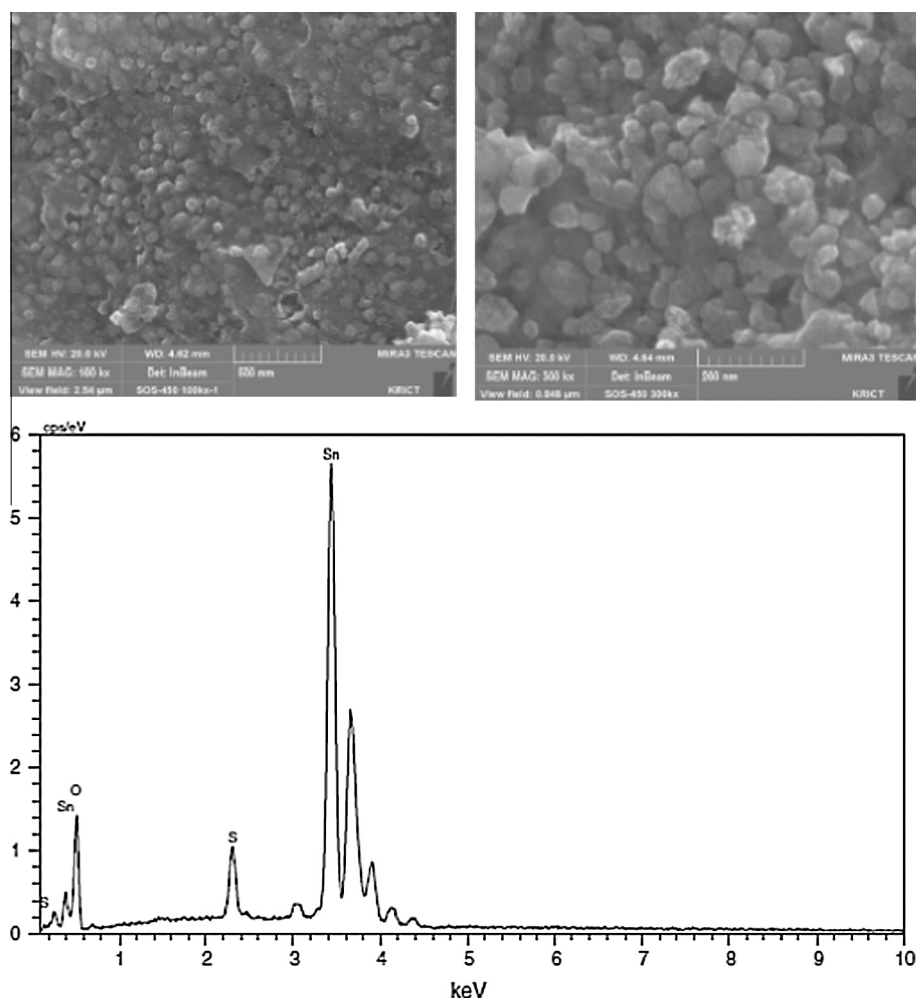


**Figure 15** SEM images and SEM-EDX spectrum of STO-450 (Dabbawala et al., 2013).

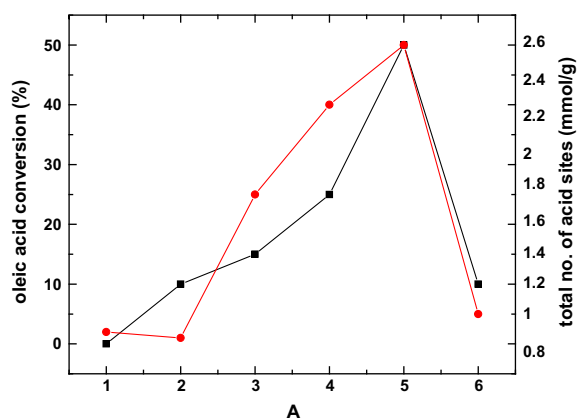


**Figure 16** Catalytic activity and total number of acid sites of the catalysts: (1)  $\text{SnO}_2$ -773 K, (2)  $\text{SO}_4^{2-}/\text{SnO}_2$ -0.45-673 K, (3)  $\text{SO}_4^{2-}/\text{SnO}_2$ -0.45-773 K, (4)  $\text{SO}_4^{2-}/\text{SnO}_2$ -0.45-873 K, (5)  $\text{SO}_4^{2-}/\text{SnO}_2$ -0.3-773 K and (6)  $\text{SO}_4^{2-}/\text{SnO}_2$ -0.15-773 K during the esterification reaction of oleic acid with ethanol (molar ratio 1:10) at 353 K, after 4 h of reaction (Moreno et al., 2011).

The research group mainly concentrated on the content of iron and tin based catalyst in the esterification reaction. The effect of different sources of iron as starting materials such as  $[\text{FeCl}_3, \text{Fe}(\text{NO}_3)_3, \text{and } \text{Fe}_2(\text{SO}_4)_3]$  in the esterification reaction was also investigated. The catalyst, 30 wt%  $\text{SO}_4^{2-}/\text{Fe}_2\text{O}_3$ - $\text{SnO}_2$ , with the highest surface area, strongest acid sites and highest NAS, was the most active. The results obtained are attributed to the interaction of sulfate ion with Sn(II) which favors the formation of two acid sites as described in Fig. 18 (Nuithitikul et al., 2011).

One interesting observation reported is that the effect was more pronounceable when the iron precursor was iron nitrate and it is due to nitrate ions which can also act as an electron withdrawing group, thereby increasing the Lewis acid strength of tin catalysts. Fig. 19 represents the comparison study of 79 wt%  $\text{SO}_4^{2-}/\text{Fe}_2\text{O}_3$ - $\text{SnO}_2$  catalysts and 79 wt%  $\text{SO}_4^{2-}/\text{SnO}_2$  catalysts activity and their stability. The authors made another observation that the sulfated tin oxide catalysts containing iron (III) oxide were having highest catalytic activity in the FFA esterification reaction and also found to be more stable. They attributed the increase in the catalytic activity of the sulfated tin oxide catalysts due to the presence of iron cations, which increased the Lewis acidity of the catalyst.

**Table 5** Textural properties of the SnO<sub>2</sub> and SO<sub>4</sub><sup>2-</sup>/SnO<sub>2</sub> catalysts (Moreno et al., 2011).

| Entry | Catalyst-sulfate (wt%)<br>Temperature (K)                     | Specific surface<br>area (m <sup>2</sup> /g) | Pore volume (cm <sup>3</sup> /g) | Pore diameter (Å) | (TGA) mmol<br>SO <sub>3</sub> /g catalyst |
|-------|---|--|----------------------------------|-------------------|---|
| 1     | SnO <sub>2</sub> (0)<br>773                                   | 62   | 0.051                            | 70                | –   |
| 2     | SO <sub>4</sub> <sup>2-</sup> /SnO <sub>2</sub> (0.45)<br>773 | 99   | 0.054                            | 25                | 0.201                                     |
| 3     | SO <sub>4</sub> <sup>2-</sup> /SnO <sub>2</sub> (0.45)<br>873 | 88   | 0.052                            | 28                | 0.137                                     |
| 4     | SO <sub>4</sub> <sup>2-</sup> /SnO <sub>2</sub> (0.30)<br>773 | 87   | 0.050                            | 28                | 0.194                                     |
| 5     | SO <sub>4</sub> <sup>2-</sup> /SnO <sub>2</sub> (0.15)<br>773 | 85   | 0.060                            | 28                | 0.129                                     |
| 6     | SO <sub>4</sub> <sup>2-</sup> /SnO <sub>2</sub> (0.45)<br>673 | 92   | 0.060                            | 26                | 0.194                                     |

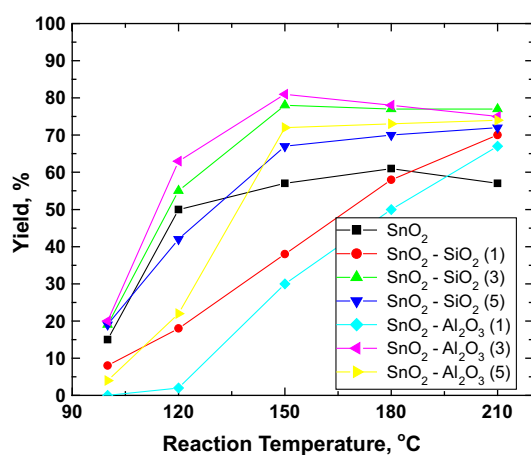


**Figure 17** Effect of reaction temperature on fatty acid methyl ester (FAME) yield using SO<sub>4</sub><sup>2-</sup>/SnO<sub>2</sub> and its sulfated mixed metal oxide. Reaction condition: methanol:oil ratio 10, catalyst loading 3 wt%, reaction time 3 h. All samples were calcined at 300 °C for 2 h (倉員貴昭, 2011).

#### 2.4. Optimized preparation of *Moringa oleifera* methyl esters

For the preparation of biodiesel, *Moringa oleifera* fatty acids were found to be potent starting material (Kafuku and Mbarawa, 2010). The SiO<sub>2</sub> enhanced sulfated tin oxide (SO<sub>4</sub><sup>2-</sup>/SnO<sub>2</sub>-SiO<sub>2</sub>) super acid solid catalyst is used for the production of biodiesel from *Moringa oleifera* oil.

#### 2.5. Transesterification reaction using biodiesel as co-solvent

For the transesterification reaction catalyzed by SO<sub>4</sub><sup>2-</sup>/SnO<sub>2</sub>-SiO<sub>2</sub>, a solid acid catalyst, Lam and his research group studied the use of biodiesel as co-solvent (Lam and Lee, 2010). They obtained a high FAME yield of 88.2% (almost 30% more than in the absence of co-solvent) when THF is used as a co-solvent in shorter reaction time (1.5 h). The research group optimized the reaction conditions as follows: 150 °C reaction temperature, 6 wt% of catalyst loading, methanol to oil ratio as 1:15.

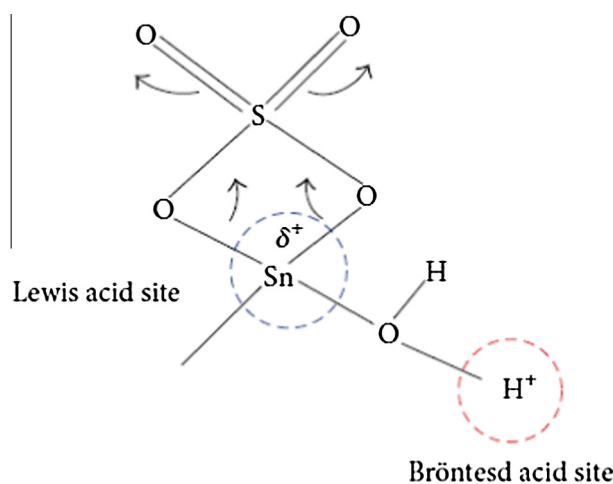


**Figure 18** Lewis and Bronsted acid sites (Nuithitikul et al., 2011).

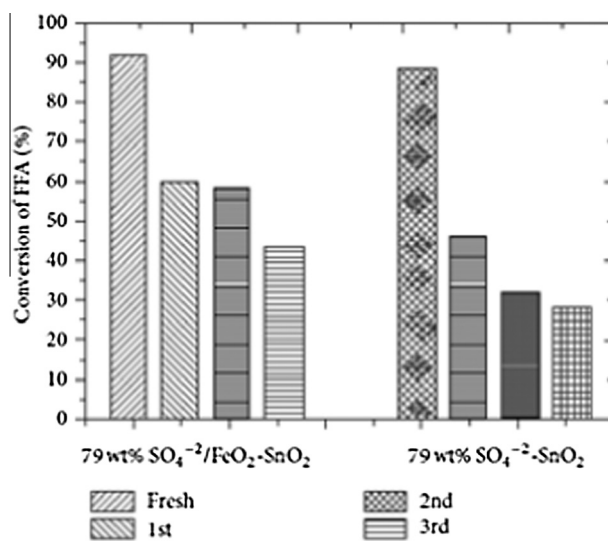


**Figure 19** Reusability of 79 wt% SO<sub>4</sub><sup>2-</sup>/Fe<sub>2</sub>O<sub>3</sub>-SnO<sub>2</sub> (III) calcined at 450 °C. Reaction time = 3 h (Nuithitikul et al., 2011).

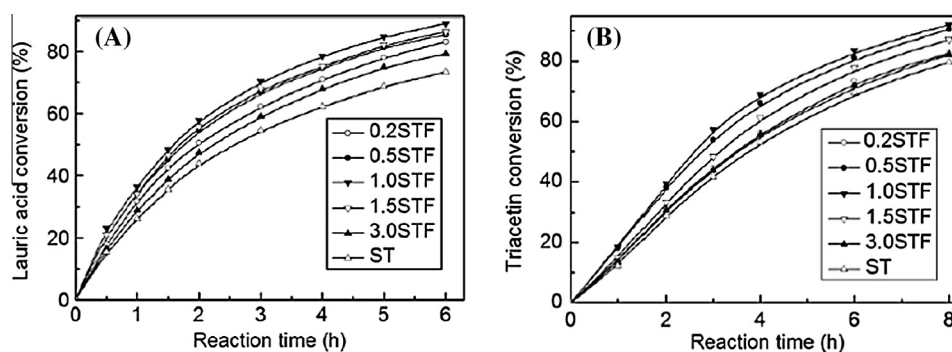


**Figure 20** (A) Esterification activity of sulfated tin oxide (STO) and sulfated tin oxide- $\text{Fe}(\text{OH})_3$  (STF) series catalysts as a function of reaction time. (B) Transesterification activity of ST and STF series catalysts as a function of reaction time (Zhai et al., 2011).

### 2.6. $\text{SnO}_2\text{-SiO}_2$ : *Croton megalocarpus* oil for bio-diesel production

Kafuku and his group investigated the conversion of non-edible oil, from *Croton megalocarpus* oil, to the methyl esters (biodiesel). The catalyst used was sulfated tin oxide enhanced with  $\text{SiO}_2$  (Kafuku et al., 2010a,b). Although the *Croton megalocarpus* oil was found to contain high free acid content, a yield up to 95% was obtained from the oil without any pretreatment step under the optimized reaction conditions. The optimized reaction conditions were as follows: temperature of 180 °C, 2 h and 15:1 methanol to oil molar ratio, 3 wt% constant catalyst concentration and 350–360 rpm stirring speed.

### 2.7. Biodiesel by catalytic reactive distillation powered by metal oxides

Kiss et al. outlined the issues associated with biodiesels present production processes as well as the properties and the use as a renewable fuel. The research group proposed a novel feasible esterification process which depends on the catalytic reactive distillation. They illustrated a metal oxide super acid solid catalyst based synthesis of the biodiesel via fatty acid esterification (Kiss et al., 2007). Among the metal catalysts prepared niobic acid, sulfated zirconia, sulfated titania, and sulfated tin oxide were found to be the best candidates.

### 2.8. Esterification and transesterification on $\text{Fe}_2\text{O}_3$ -doped sulfated tin oxide catalysts

A variety of  $\text{Fe}_2\text{O}_3$  (0.2–3%) doped sulfated tin oxide solid catalysts were prepared by employing the co-precipitation process followed by sulfation and calcination methods. Zhai et al. observed that by addition of small amounts of  $\text{Fe}_2\text{O}_3$  to the STO, the number of active/strong acid sites was increased and hence the  $\text{Fe}_2\text{O}_3$  doped STO catalysts were found to be more active, for the esterification of lauric acid with methanol and transesterification of triacetin with methanol, than the undoped ones (Zhai et al., 2011). The STO catalyst containing 1% of  $\text{Fe}_2\text{O}_3$  exhibits highest activity for the biodiesel production as illustrated in Fig. 20.

### 2.9. Esterification and transesterification on $\text{Al}_2\text{O}_3$ -doped sulfated tin oxide solid acid catalysts

Zhai research group prepared a series of  $\text{Al}_2\text{O}_3$  (0.5–3%) doped sulfated tin oxide catalysts by using the co-precipitation process. They investigated the catalytic activity of these catalysts in the esterification reaction of lauric acid with methanol and transesterification of triacetin with methanol (Zhai et al., 2010). The results showed that the catalytic activity improved markedly by the addition of  $\text{Al}_2\text{O}_3$  to STO. The remarkable activity of the catalyst was due to the increase in the number of acid sites. The sulfated tin oxide catalyst doped with 1 mol% of  $\text{Al}_2\text{O}_3$  found to exhibit highest activity. The lauric acid esterification was 92.7% and triacetin transesterification was 91.1%, with the help of this catalyst, after 6 h and 8 h respectively.

### 2.10. Synthesis of sulfated silica-doped tin oxides and their high activities in transesterification

Xiao et al. synthesized a series of sulfated tin oxide catalysts doped with silica with large surface areas (113–188  $\text{m}^2/\text{g}$ ) by employing hydrothermal synthesis, sulfation and calcination methods. These catalysts were characterized by XRD, FT-IR, TEM, nitrogen isotherms, and TG techniques. The authors observed that these catalysts are composed of tetragonal nanocrystalline tin oxides and amorphous silica. These silica doped sulfated tin oxide catalysts found to show excellent catalytic activity for the transesterification of triacetin with methanol when compared with the conventional sulfated tin oxide catalysts (Du et al., 2008).

### 2.11. Application of sulfated tin oxide in transesterification and bio-diesel production

The doping of sulfated tin oxide with aluminum resulted in better catalytic activity and acidity than the zirconia and titanium doping on sulfated tin oxide as reported by Guo et al. (2008). The incorporation of aluminum on  $\text{SO}_4^{2-}/\text{SnO}_2\text{-Al}_2\text{O}_3$  via co-condensation method at Sn/Al ratio of 9:1 and calcined at 500 °C, gave the best activity. From the FT-IR results, it was observed that the active sites are due to Sn, which was chelated with sulfuric acid. By introducing aluminum, the number of the sulfate groups attached on the surface increased. And

**Table 6** Activation energy for NH<sub>3</sub> desorption, BET surface, and crystal size for super acid sulfated tin oxide catalysts (Lam et al., 2009).

| Catalyst activation  | Activation energy (kJ/mol) | Correlation factor ( $R^2$ ) | BET (surface area) | Crystal size (nm) |
|--|----------------------------|------------------------------|--------------------|-------------------|
| SnO <sub>2</sub>   | 5.69                       | 0.9540                       | 8.32               | 60.7              |
| SO <sub>4</sub> <sup>2-</sup> /SnO <sub>2</sub> , 300 °C                                 | 7.25                       | 0.9687                       | 6.77               | 42.9              |
| SO <sub>4</sub> <sup>2-</sup> /SnO <sub>2</sub> , 400 °C                                 | 7.18                       | 0.9715                       | –                  | 59.6              |
| SO <sub>4</sub> <sup>2-</sup> /SnO <sub>2</sub> , 500 °C                                 | 6.01                       | 0.9877                       | –                  | 62.0              |
| SO <sub>4</sub> <sup>2-</sup> /SnO <sub>2</sub> –SiO <sub>2</sub> , 300 °C               | 9.40                       | 0.9991                       | 13.90              | 47.7              |
| SO <sub>4</sub> <sup>2-</sup> /SnO <sub>2</sub> –Al <sub>2</sub> O <sub>3</sub> , 300 °C | 7.51                       | 0.9925                       | 14.04              | 45.4              |

the observations made from thermogravimetric analysis, further strengthened the catalyst's activity. Lam et al. observed a yield of 92.3% with SO<sub>4</sub><sup>2-</sup>/SnO<sub>2</sub>–SiO<sub>2</sub> with a weight ratio of 3:1 at 150 °C, 3 wt% of catalyst, and 15:1 methanol to oil molar ratio in 3 h (Lam et al., 2009).

Calcination temperature was pivotal for these catalytic reactions (300 °C). BET surface area and crystal size of sulfated tin oxide catalysts were also investigated along with the activation energy of the NH<sub>3</sub> desorption super acid sulfated tin oxide catalyst as shown in Table 6. The acid acidic strength of catalyst can be measured from the activation energy of the NH<sub>3</sub> desorption.

#### 2.11.1. The heterogeneous transesterification of *Jatropha curcas* oil

*Jatropha curcas* seeds contain non-edible oil yielding excellent results in the biodiesel industry. It consists of a high free fatty acid content that can be converted into methyl esters by transesterification using a basic catalyst. The sulfated tin oxide enhanced with SiO<sub>2</sub> (SO<sub>4</sub><sup>2-</sup>/SnO<sub>2</sub>–SiO<sub>2</sub>), a super acid solid catalyst, was used by Kafuku et al. to prepare methyl esters from the *Jatropha curcas* oil (Kafuku et al., 2010a,b). They set up the experiments using the response surface central composite design (CCD). The reaction parameters considered were the reaction temperature, reaction period and methanol to oil ratio. CCD was used to investigate linear, quadratic and cross-product effects of the given reaction parameters on the yield of *jatropha* methyl esters. The value of  $\alpha$  was fixed at 2. A maximum yield (97%) of methyl ester was obtained at a temperature of 180 °C, 1:15 M ratio of methanol and oil for a reaction period of 2 h.

#### 2.11.2. Esterification of free fatty acids in crude palm oil

The production of biodiesel from the crude palm oil using the homogeneous base catalyst contains large amounts of free fatty acid (FFA) and it also results in the soap formation and thereby reducing the yield of biodiesel. To overcome these problems, the free fatty acids need to be esterified to their esters by using an acid catalyst prior to alkaline catalyzed transesterification. A number of aluminum doped sulfated tin oxide catalysts were synthesized by using different aluminum precursors/starting materials (Prasitturattanachai and Nuihitikul, 2013). From the results, it was observed that the different aluminum precursors gave different activities of catalysts. The esterification reaction of free fatty acids with methanol using these catalysts found to follow the first-order kinetics.

#### 2.11.3. Synthesis of biodiesel via acid catalysis

The sulfated tin oxide catalysts, prepared from *m*-stannic acid, were found to exhibit higher catalytical activity than the

**Table 7** Esterification of *n*-octanoic acid with methanol at 175 and 200 °C (Furuta et al., 2004a,b).

| Catalyst | Conversion (%) |        |
|----------|----------------|--------|
|          | 175 °C         | 200 °C |
| WZA      | 94             | 100    |
| SZA      | 99             | 100    |
| STO      | 100            | 100    |

sulfated zirconia catalysts for the esterification reaction of *n*-octanoic acid with methanol at temperature < 150 °C. The high activity of the catalyst is due to the increase in super acid strength (Lotero et al., 2005).

#### 2.11.4. Biodiesel fuel production in fixed bed reactor under atmospheric pressure

For the esterification of *n*-octanoic acid and for transesterification of soya bean oil with methanol, numerous sulfated tin oxide super acid solid catalysts were synthesized and analyzed by Furuta et al. (2004a,b).

The very important point for the biodiesel production is the catalytic activity of the catalyst in the esterification of carboxylic acid. It is mainly because of the existence of free fatty acids. Hence, the esterification of *n*-octanoic acid with methanol to the corresponding ester was done under the same reaction conditions as that of the transesterification of soybean oil. The yields of the esterification reaction are illustrated in Table 7. A yield of 100% was obtained at temperatures above 175 °C by the tungstated zirconia–alumina (WZA), sulfated tin oxide (STO), and sulfated zirconia–alumina (SZA) catalysts. No by-products were detected in this catalysis. The probable reason for the excellent catalytic activity and least by-product formation could be due to the acidic nature of the catalyst.

For the esterification of *n*-octanoic acid the STO showed especially high activity due to its strong acidity.

#### 2.11.5. STO-Catalyzed esterification and etherification reactions

Another important reaction that proceeds in the acidic medium is esterification. Sulfated tin oxide catalysts were synthesized by Furuta and coworkers using SnCl<sub>4</sub> and SnO<sub>2</sub> precursors such as tin oxide gel and *m*-stannic acid, after treatment with sulfuric acid. They investigated catalytic activity on the esterification and etherification reactions (Furuta et al., 2004a,b). STO-1 was the sulfated tin obtained by the route SnCl<sub>4</sub> and STO-2 was the sulfated tin obtained by route SnO<sub>2</sub>. Additionally, they also prepared the sulfated zirconium catalyst (SZ). All catalysts were found to display tetragonal

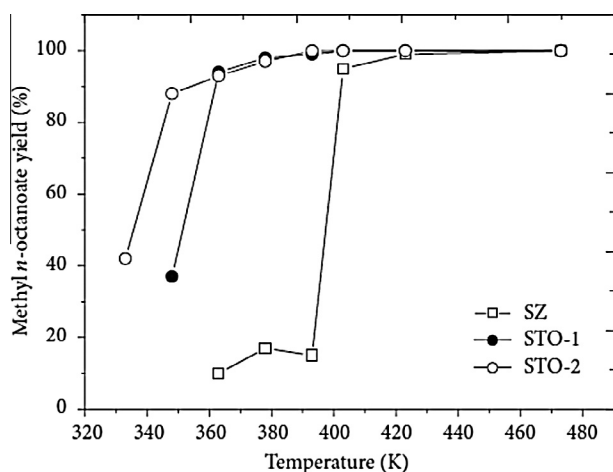


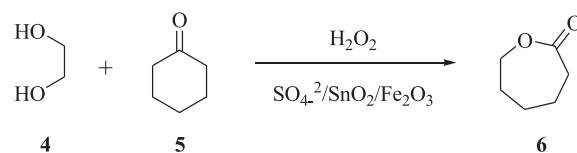
**Figure 21** Octanoic acid esterification with methyl alcohol over STO-1, STO-2, and SZ for 20 h (Reaction conditions: 4.0 g of catalyst, methanol:octanoic acid molar ratio 4.5:1.) (Furuta et al., 2004a,b).

crystalline structure after the characterization. Fig. 21 shows the kinetic curves obtained in the octanoic acid esterification with methyl alcohol using the sulfated tin and zirconium oxides catalysts, in 333–473 K range of temperature, for a reaction time of 20 h (Furuta et al., 2004a,b). At lower temperatures the tin catalysts STO-1 and STO-2 were highly effective in achieving high conversion values. The authors highlighted that even in the presence of water the ability of sulfated tin oxide catalysts remains stable throughout reaction.

### 3. Catalytic application of sulfated tin oxide in organic synthesis

#### 3.1. Synthesis of 7-hydroxy-4-methyl coumarin using Pechmann condensation method

Different sulfate content (5–30% by weight) containing nanostructure sulfated tin oxides was synthesized from the hydroxylated tin oxide (obtained from precipitation method) and  $\text{SO}_4^{2-}$  species of the sulfuric acid. At the temperatures 400, 500, and 600 °C, the so prepared sulfated tin oxide catalysts were calcinated. These catalysts were analyzed in the solvent free synthesis of 7-hydroxy-4-methyl coumarin from ethyl acetoacetate: resorcinol (molar ratio 2:1) at 120 °C by using the Pechmann condensation methodology (Ahmed et al., 2013). The FT-IR spectra in pyridine of these catalysts clearly indicated the existence of the Lewis acid sites and the Bronsted acid sites on the surface of the catalyst. It was also observed that the percentage of yield of product increased with increase in the acidity of the catalyst surface. By maintaining a calcination temperature of



**Scheme 2** Acetalization of cyclohexanone.

400 °C and 25 weight percentage sulfate content, a maximum yield of the 7-hydroxy-4-methyl coumarin was obtained as shown in Scheme 1.

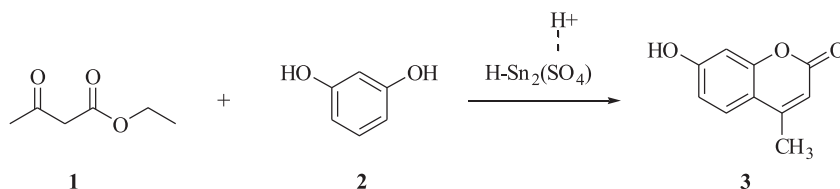
#### 3.2. Baeyer–Villiger oxidation and acetalization of cyclic ketones

The Baeyer–Villiger reaction, which is also known as Baeyer–Villiger oxidation, is an important reaction, wherein introduction of oxygen atom in the ring system takes place. This can be carried out in the presence of hydrogen peroxide, peracids, such as MCBPA, and a Lewis acid. A variety of iron doped sulfated tin oxide solid acid catalysts were prepared with different amounts of iron and by utilizing the co-condensation, sulfation and calcination methods, respectively. These iron doped catalysts were found to be more active than the undoped catalysts in acetalization reactions of 4-*tert*-butylcyclohexanone and diols (Yang et al., 2012). The acetalization reaction between several ketones and diols was analyzed with these Fe-doped catalysts and Fe/Sn molar ratio of 0.5. Wang et al. also studied the amount of catalyst used and the reaction times by these catalysts in the acetalization reaction. It was also observed that these doped catalysts showed high performance in the Baeyer–Villiger oxidation of cyclic ketones in addition to the acetalization reaction as depicted in Scheme 2. This improved catalytic performance can be attributed to the presence of acidic sites, important for the above transformation to take place.

#### 3.3. Synthesis of 2,4,5-triaryl-1H-imidazole derivatives

The 2,4,5-triaryl-1H-imidazole compounds have drawn the attention of synthetic chemists and biologists because of their widespread biological applications such as proton pump inhibitors (omeprazole), antiulcerative agents (cimetidine), and benzodiazepine antagonist. Trifenagrel, 2,4,5-triaryl-1H-imidazole compound, was found to reduce the platelet aggregation in several animal species and humans (Wiglenda et al., 2005).

Using three component one-pot condensation reaction between benzyl/benzoin, substituted aromatic aldehydes, and ammonium acetate in ethanol/water solvent system (1:1), reflux conditions, in the presence of the sulfated tin oxide



**Scheme 1** STO-Catalyzed synthesis of 7-hydroxy-4-methyl coumarin.

catalyst, the synthesis of 2,4,5-triaryl-1*H*-imidazoles was achieved in excellent yields (Dake et al., 2012). This condensation has advantages such as mild reaction conditions, fast rate, excellent product yield, green and reusability of the catalysts. As demonstrated in Scheme 3, this methodology maintains atom economy and it is environment friendly protocol.

### 3.4. Dehydration of xylose

D-xylose is a cheap source and starting material for the synthesis of important chemicals such as xylitol, ethanol, furfuryl alcohol, furfural and furan. Among all the above derivatives of D-xylose, furfural is very important chemical for the wide range production of non-petroleum derived chemicals. It is also useful as a raw material for the preparation of furan derivatives (Corma et al., 2007).

As depicted in Scheme 4, numerous sulfated metal oxides were tested under milder conditions as solid catalysts for the preparation of the furfural from D-xylose (Suzuki et al., 2011). Based on the observations, it was noted that the sulfated tin oxide displayed high catalytic activity toward the dehydration of xylose. Corma et al. also investigated the effect of the sulfate content and the calcination temperature on the yield of the reaction. One more advantage of the methodology developed is the reusability of the sulfated tin oxide solid acid

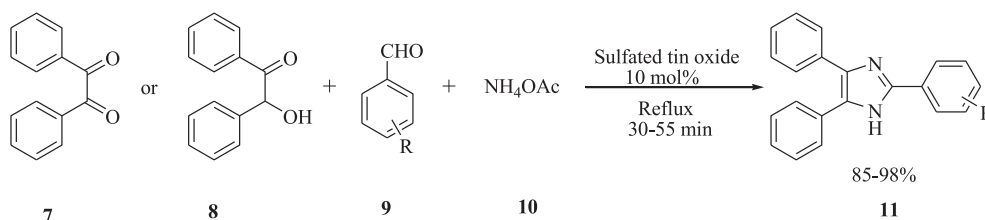
catalyst. The acidic properties of the sulfated tin oxide catalyst were analyzed by an *in situ* FT-IR (CO adsorbed sample).

Among the variety of the catalysts prepared, the  $\text{SO}_4^{2-}/\text{SnO}_2$  displayed the maximum catalytic activity in the dehydration of xylose with a yield of 27% as mentioned in Table 8. Based on the results obtained, the sulfated tin oxide was chosen as the best catalyst for the dehydration reaction of xylose or the preparation of the furfural.

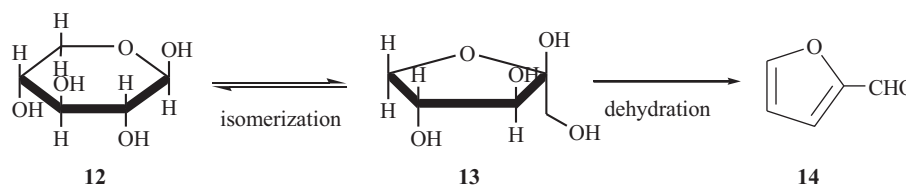
It is considered that the Lewis acid sites (LASs) and the Bronsted acid sites (BASs) present on the  $\text{SO}_4^{2-}/\text{SnO}_2$  catalyst surface could function as active site independently. As shown in Scheme 4, the isomerization of xylose to xylulose takes place by Lewis acid sites and the dehydration of xylulose to form furfural takes place by the Bronsted acid sites.

### 3.5. Friedel–Crafts acylation of toluene

Using different amounts of sulfate, the sulfated tin oxide catalysts were prepared. The catalyst surface acidity was determined by using the TGA/Pyridine sample. The acid strength of the catalyst was analyzed with potentiometric titration with *n*-butylamine in non-aqueous media. To investigate the catalytic activity, the Friedel–Crafts acylation of toluene as represented in Scheme 5, the product was achieved with the prepared sulfated catalysts (El-Sharkawy and Al-Shihry,



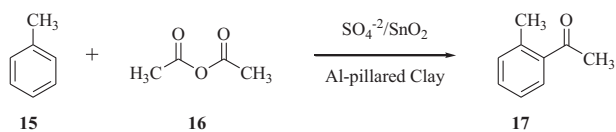
Scheme 3 STO-Catalyzed synthesis of 2,4,5-triaryl-1*H*-imidazole derivatives.



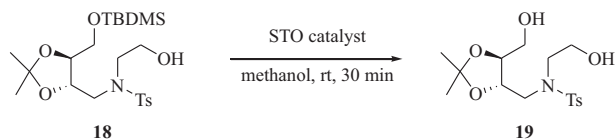
Scheme 4 Dehydration of xylose over sulfated tin oxide catalyst.

Table 8 Structural properties and catalytic performances of various SMOs (Suzuki et al., 2011).

| Catalyst                                 | $S_{\text{BET}}$ ( $\text{m}^2/\text{g}$ ) | $\text{SO}_4^{2-}$ content (mmol/g) | Conv. (%) | Yield (%) |
|--|--|-------------------------------------|-----------|-----------|
| No catalyst                              | –  | –                                   | 13.4      | 2.2       |
| $\text{H}_2\text{SO}_4$                  | –  | –                                   | 22.5      | 18.7      |
| $\text{SO}_4^{2-}/\text{Al}_2\text{O}_3$ | 209  | 0.92                                | 7.1       | 2.4       |
| $\text{SO}_4^{2-}/\text{SiO}_2$          | 147  | 0.04                                | 2.2       | 0.9       |
| $\text{SO}_4^{2-}/\text{TiO}_2$          | 126  | 0.64                                | 38.6      | 16.8      |
| $\text{SO}_4^{2-}/\text{Fe}_2\text{O}_3$ | 67   | 0.37                                | 16.1      | 1.1       |
| $\text{SO}_4^{2-}/\text{ZrO}_2$          | 152  | 0.39                                | 20.7      | 9.3       |
| $\text{SO}_4^{2-}/\text{Nb}_2\text{O}_5$ | 39   | 0.58                                | 19.7      | 7.8       |
| $\text{SO}_4^{2-}/\text{SnO}_2$          | 127  | 0.64                                | 57.3      | 26.6      |
| $\text{SO}_4^{2-}/\text{HfO}_2$          | 158  | 0.22                                | 41.7      | 9.8       |



**Scheme 5** STO-Catalyzed Friedel-Crafts acylation of toluene.



**Scheme 6** STO-Catalyzed deprotection of *tert*-butyldimethylsilyl ether.

2010). A higher yield of the acylation products was obtained with sulfated tin oxide than  $\text{Al}^{3+}$ -impregnated sulfated zirconia, since STO has greater acidity and higher acid strength. It was also observed that the sulfated tin oxide, with sulfate loading was 10 wt%, was found to show higher efficiency and higher acidity for the acylation of toluene reaction. It was also reported that among the structural characteristics, the acidity of the catalyst and its catalytic performance were closely related.

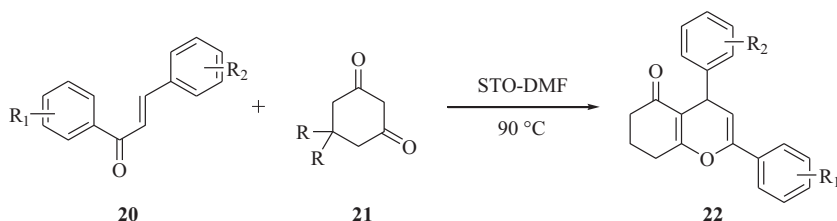
### 3.6. Deprotection of silyl ether

The *tert*-butyldimethylsilyl ether can be highly selectively deprotected using sulfated tin oxide as an efficient solid catalyst at room temperature as illustrated in **Scheme 6** (Bhure et al., 2008). Numerous TBDMS ethers with acid labile groups are converted to silyl deprotected compounds using this protocol, in exceptional yields, at room temperature with very short reaction times.

### 3.7. Synthesis of 2,4-diphenyl-4,6,7,8-tetrahydrochromen-5-one

2,4-diphenyl-4,6,7,8-tetrahydrochromen-5-ones can be obtained by the reaction of  $\alpha$ ,  $\beta$ -unsaturated carbonyl compounds with 1,3-cyclohexanedione, under heating conditions, using sulfated tin oxide in good to excellent yields as demonstrated in **Scheme 7** (Sarda et al., 2007). The advantage of the methodology is that the catalyst can be recovered by simple filtration method. It is observed that the catalyst can be reused for several times in subsequent reactions with same efficiency.

Among the numerous solvents analyzed for the reaction the sulfated tin-DMF solvent was found to be appropriate mainly due to shorter reaction time and simple workup procedure.



**Scheme 7** STO-Catalyzed synthesis of 2,4-diphenyl-4,6,7,8-tetrahydro chromen-5-ones.

**Table 9** Synthesis of 7,7-dimethyl-2,4-diphenyl-4,6,7,8-tetrahydro chromen-5-one (Sarda et al., 2007).

| Entry | Solvent                         | Temp. (°C) | Time (h) | Yield (%)   |
|-------|---------------------------------|------------|----------|-------------|
| 1     | Toluene                         | Reflux     | 12       | 70          |
| 2     | $\text{CH}_3\text{CN}$          | Reflux     | 14       | 75          |
| 3     | $\text{C}_2\text{H}_5\text{OH}$ | Reflux     | 13       | 70          |
| 4     | $\text{CH}_3\text{OH}$          | Reflux     | 14       | 65          |
| 5     | DMF                             | RT         | 38       | No reaction |
| 6     | DMF                             | 120 °C     | 4.5      | 90          |
| 7     | DMF                             | 90 °C      | 7        | 92          |

The catalyst required longer reaction times using other organic solvent systems as shown in **Table 9**.

### 3.8. C3-alkylation and O-alkylation of 4-hydroxycoumarins

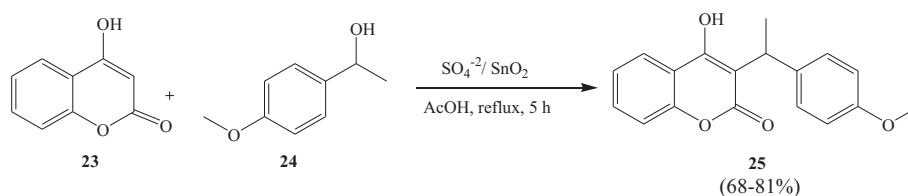
Narayana et al. utilized sulfated tin oxide solid acid catalyst as an excellent catalyst for the C3-alkylation and O-alkylation of 4-hydroxycoumarins, in good yields, using the allylic, benzylic alcohols/and corresponding acetates respectively, under reflux conditions in acetic acid (Narayana et al., 2012). The  $\text{SO}_4^{2-}/\text{SnO}_2$  catalyst is found to be efficient and reusable for several subsequent reactions.

This methodology was found to be a mild synthetic and straightforward route for the preparation of the multi-substituted pyranocoumarins. These novel compounds can be easily obtained by treating secondary benzyl acetates with 4-hydroxycoumarin under the above optimized conditions in good yields. From **Schemes 8** and **9**, authors adopted this protocol for the formation of the new C—O bonds.

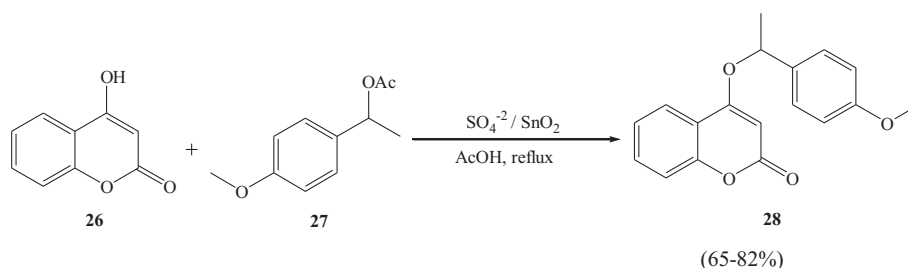
As depicted in **Fig. 22**, the above reaction is found to take place through a tandem sequence of steps. The authors also proposed a mechanism involving the Bronsted acid site (C-3 alkylation) of the sulfated tin oxide catalyst, which will act as an alkylating species, whereas in case of O-alkylation, the Lewis acid site activates the carbonyl group of acetate and makes it as a leaving group and then formed carbocation reacts with enolic hydroxide leaving acetic acid as a by-product.

### 3.9. Efficient one-pot synthesis of 7,8-dihydro-2H-chromen-5-ones

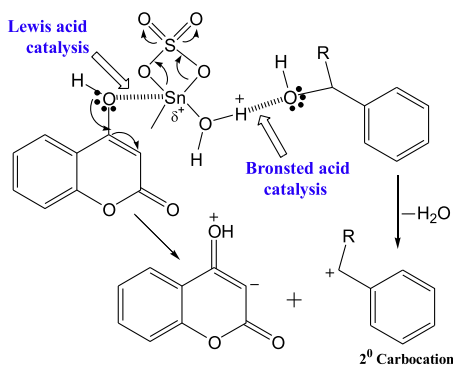
Narayana et al. synthesized STO catalyzed one-pot synthesis of 7,8-dihydro-2H-chromen-5-ones by formal [3 + 3] cycloaddition (**Scheme 10**) strategy under milder reaction conditions in good yields. Similarly, STO was found to be an efficient catalyst for the synthesis of 1,8-dioxo-octahydroxanthenes *via* a



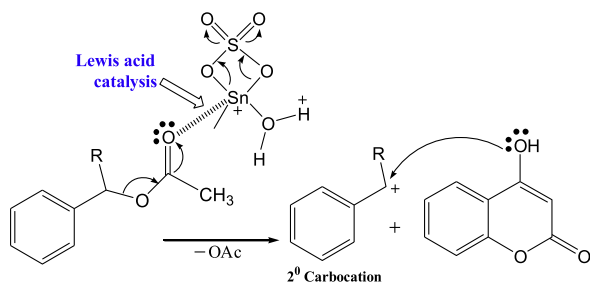
**Scheme 8** STO-Catalyzed C3-alkylation of 4-hydroxycoumarins.



**Scheme 9** STO-Catalyzed O-alkylation of 4-hydroxycoumarins.

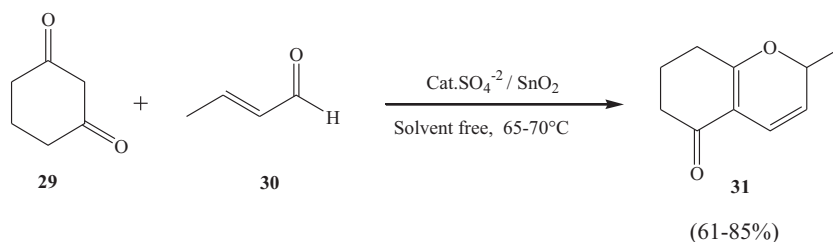


**Mechanism for C3-Alkylation via Bronsted and Lewis acid Catalysis using STO**



**Mechanism for O-Alkylation via Lewis acid Catalysis using STO**

**Figure 22** Mechanism for C and O-alkylation using STO.



**Scheme 10**  $\text{SO}_4^{2-}/\text{SnO}_2$ -Catalyzed synthesis of 7,8-dihydro-2H-chromene-5(6H)-ones.

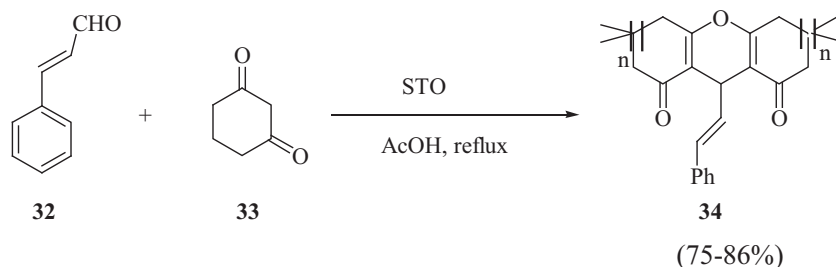
Knoevenagel condensation (Scheme 11) under similar reaction conditions. The main advantage of these synthesis protocols is that the catalyst can be used again for numerous times without losing its catalytic efficiency (Narayana et al., 2013).

The [3 + 3] cycloaddition reaction between 1,3-dicarbonyl compounds and  $\alpha,\beta$ -unsaturated aldehydes resulted in the formation of the corresponding 2H-pyran motif. From the synthetic perspective, this kind of protocol allows the formation of rings and multiple bonds.

A 2:1 M ratio of aldehydes and diketones, under the STO catalytic reaction conditions, reacts together to form 1,8-dioxo-octahydroxanthenes (Scheme 11). The Knoevenagel condensation between the enol derivative of  $\beta$ -diketone and electrophilic carbonyl of enal resulted in the formation of oxa-intermediate, which in turn underwent [3 + 3] electrocycloaddition to give the product. The probable mechanism is given in Fig. 23.

### 3.10. Facile transesterification of ketoesters

As demonstrated in Scheme 12, the sulfated tin oxide solid acid catalyst was found to be highly efficient in the transesterification reactions of the ketoesters (Chavan et al., 1996). This methodology highly contradicts the earlier reported protocols with regard to the usage of the molecular sieves in large excess amounts than the stoichiometric amounts of DMAP for the smooth reaction/exchange (Gilbert and Kelly, 1988).



**Scheme 11**  $\text{SO}_4^{2-}/\text{SnO}_2$ -Catalyzed synthesis of 1,8-dihydro-octahydroxanthenes.

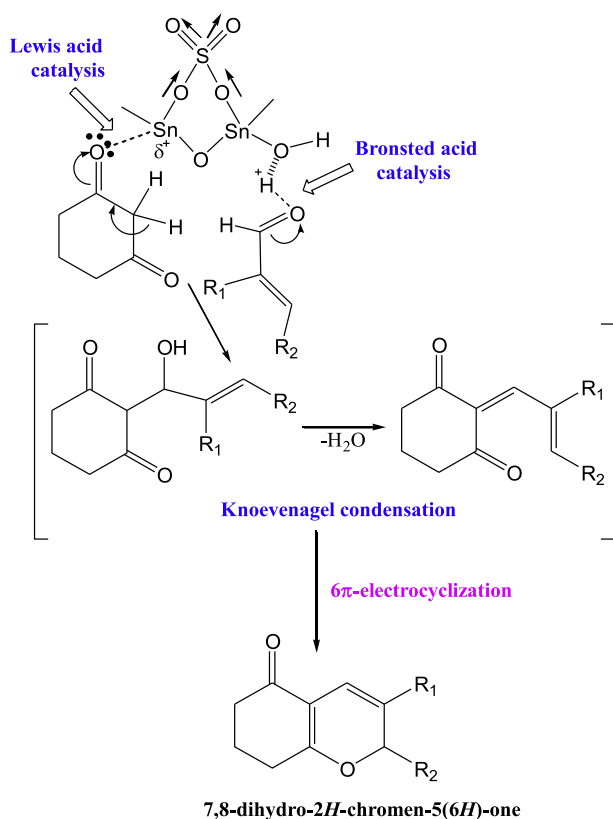
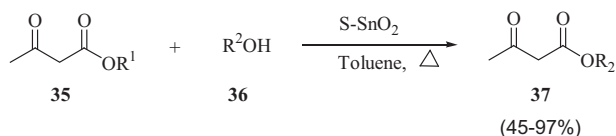


**Figure 23** Possible formation mechanism of 1,8-dioxo-octahydroxanthene.



**Scheme 12** STO-Catalyzed transesterification reactions of the ketoesters.

Employing Chavan's synthetic route even the tertiary butyl esters could be synthesized, which clearly demonstrated the generality and superiority of the methodology. It was not possible to prepare the *tert*-butyl ester with the earlier reported protocols.

The above reported methodology is highly effective and selective toward the  $\beta$ - and  $\gamma$ -ketoesters and it is not applicable to the normal esters. The carbonyl group improves the reactiv-

ity of the ester by chelation with the oxide and it is vital for the success of the reaction. Hence, it indicates the high selectivity and transesterification of ketoesters.

### 3.11. Aldol condensation and benzoylation

Highly active solid sulfated tin oxide catalyst was prepared from the reaction of aqueous sulfuric acid with tin oxide gel, obtained from the hydrolysis of  $\text{SnCl}_4$  and aqueous ammonia acetate solution washing, followed by calcination. It was reportedly observed from the differential thermal studies, suggests that the acetate ion on the catalyst surface is swapped by the sulfate ion. When a comparative study between sulfated tin oxide and sulfated zirconia was carried out, the acidic strength of the sulfated tin oxide was found to be much higher than the sulfated zirconia as evident from the temperature-programmed desorption technique using argon gas. The activation energy of Ar desorption by the sulfated tin oxide was  $10.6 \text{ kJ mol}^{-1}$  in comparison with  $9.3 \text{ kJ mol}^{-1}$  by the sulfated zirconia. The sulfated tin oxide catalyst displayed greater efficiency than the sulfated zirconia toward Mukaiyama aldol condensation between 1-trimethylsilyloxy-1-cyclohexane and benzaldehyde and benzoylation of toluene with benzoic anhydride and the skeletal isomerization of *n*-pentane (Matsushashi et al., 2001a, b) (Scheme 13).

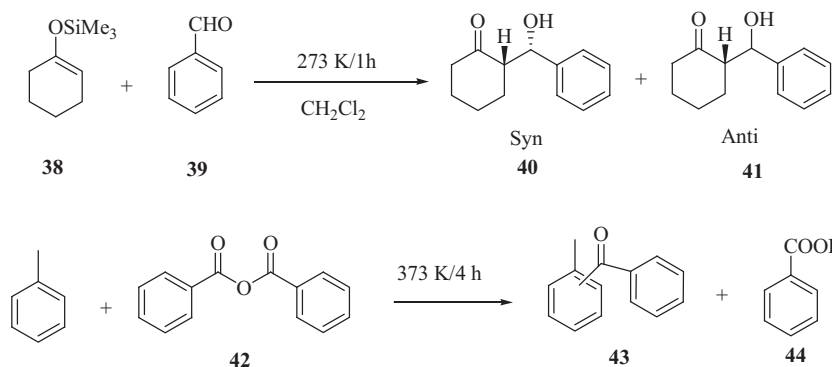
The acid strength estimation by Ar-TPD for the sulfated tin oxide has higher value than that of sulfated zirconia (Table 10). It displayed activities superior than that of sulfated zirconia for the isomerization of *n*-pentane.

### 3.12. Synthesis of structurally diverse $\beta$ -acetamido ketones and aryl-14*H*-dibenzo(*a,j*)xanthenes

Under the microwave energy irradiation, the sulfated tin oxide solid acid catalysts were found to be excellent for the synthesis of aryl-14*H*-dibenzo(*a,j*)xanthenes and structurally diverse  $\beta$ -acetamido ketones under environment friendly conditions as described in Schemes 14 and 15. The great advantages of this synthetic protocol are that both the synthetic products were obtained in excellent yields with high purity and shorter reaction times (Naik et al., 2009).

### 3.13. Selective dehydration of sorbitol

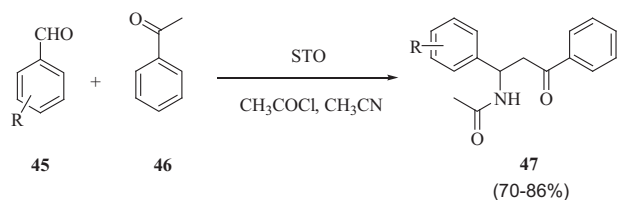
Employing the thermal decomposition of the stannous sulfate, numerous sulfated tin oxide catalysts containing different sulfur amounts (1–8 wt%) were synthesized. These STO catalysts were analyzed in the solvent-free liquid phase dehydration of



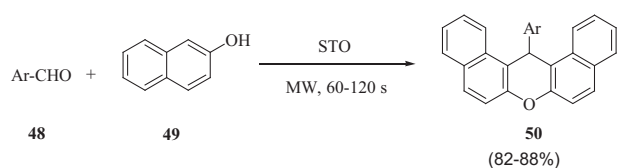
**Scheme 13** Mukaiyama Aldol reaction of 1-trimethylsilyloxy-1-cyclohexene with aldehyde and Friedel–Crafts benzoylation of toluene with benzoic anhydride.

**Table 10** Catalytic activities in Aldol condensation and benzoylation (Matsuhashi et al., 2001a,b).

| Catalyst  | Aldol condensation |                       | Benzoylation                             |                 |
|---|--------------------|-----------------------|--|-----------------|
|   | Yield (mol%)       | Syn:anti <sup>a</sup> | Yield/mmol (g of catalyst) <sup>-1</sup> | Ortho:meta:para |
| SO <sub>4</sub> <sup>2-</sup> /SnO <sub>2</sub> | 100                | 44:56                 | 2.52                                     | 27:5:68         |
| SO <sub>4</sub> <sup>2-</sup> /ZrO <sub>2</sub> | 52                 | 33:67                 | 2.37                                     | 37:3:60         |

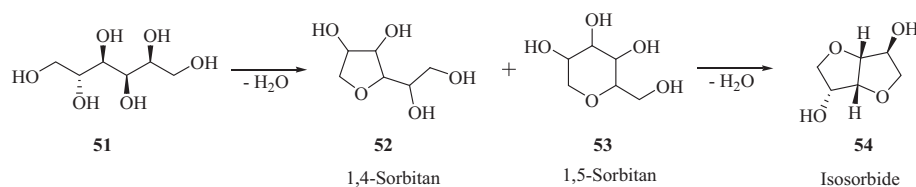


**Scheme 14** Sulfated tin oxide catalyzed one pot synthesis of  $\beta$ -acetamido ketones.



**Scheme 15** Sulfated tin oxide catalyzed synthesis of aryl-14H-dibenzo(a,j)xanthenes.

sorbitol (Dabbawala et al., 2013). It is observed that the isosorbide selectivity and the sulfur content in the catalyst were affected by the calcination temperature. As illustrated in



**Scheme 16** Dehydration of sorbitol to isosorbide.

**Scheme 16**, the sulfated tin oxide showed excellent catalytic activity in the production of isosorbide from sorbitol (in around 65% yield in 2 h at 180 °C) when compared with the sulfated zirconia. The authors also investigated the effect of amount of catalyst, reaction time and reaction temperature on the selectivity and yield of the product. Here also the catalyst can be regained from the reaction mixture and be reemployed with same efficiency in several consecutive reactions.

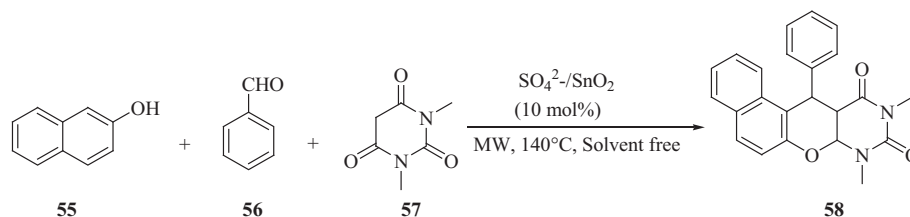
### 3.14. One-pot synthesis of naphthopyranopyrimidines

Naphthopyranopyrimidine and its derivatives play an essential and promising role in medicinal and pharmaceutical industry (Radi et al., 2009). **Scheme 17** demonstrates a one-pot three component coupling between aromatic aldehydes,  $\beta$ -naphthol, and 1,3-dimethylbarbituric acid to yield the naphthopyranopyrimidine derivatives using the sulfated tin oxide as catalyst (Alam et al., 2014). It is a mild and rapid methodology developed under solvent free conditions with shorter reaction times and excellent yields of the products (72–96%). The significant advantages of this methodology are clean reaction, simple operation, easy workup and high yield of product.

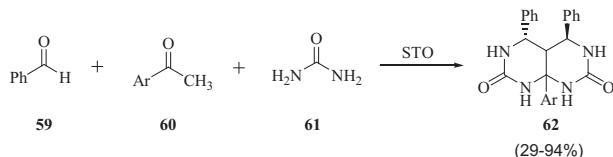
Some more advantages of the sulfated tin oxide are that it is stable to heat, air, and moisture, easy separation, environment friendly, and less corrosive toward reactors and containers.

### 3.15. Synthesis of pyrimidopyrimidines

**Scheme 18** demonstrates the synthesis of 4,5,8a-triarylhexahydro-dropyrimido[4,5-*d*]pyrimidine-2,7-(1*H*,3*H*)-diones, the Biginelli type compounds, by employing a one-pot three component reaction between benzaldehyde, aromatic ketone and urea under sulfated tin oxide catalysis (Magar et al., 2013). The promising and main advantages of the methodology are shorter reaction times, high yield, and reusability of the catalyst. Both Bronsted and Lewis acidic sites of STO were



**Scheme 17** STO catalyzed synthesis of naphthopyranopyrimidines.



**Scheme 18** STO catalyzed synthesis of pyrimidopyrimidines.

schematically shown to be active for the success of the reaction.

### 3.16. Catalytic pyrolysis of cellulose: synthesis of light furan compounds

For the synthesis of medicine, food, fuel additives, resins, and other products, the furan compounds are widely used as organic solvents/reagents, which make them value-added chemicals. The fast pyrolysis of cellulose followed by catalytic cracking of the pyrolysis vapor yields a variety of furan compounds, which were identified by the on-line analysis of pyrolysis vapors by utilizing pyrolysis–gas chromatography/mass spectrometry (pY–GC/MS). For the catalytic cracking of the pyrolysis vapor, three sulfated metal oxides ( $\text{SO}_4^{2-}/\text{TiO}_2$ ,  $\text{SO}_4^{2-}/\text{ZrO}_2$  and  $\text{SO}_4^{2-}/\text{SnO}_2$ ) were employed. By altering the prepared catalysts, the dissemination of the pyrolytic products was changed significantly. Products, such as levoglucosan and hydroxyacetaldehyde, which are considered as important primary pyrolytic outcomes were appreciably diminished or even completely eliminated by varying different catalysts.

At the same time, three light furan compounds (furan, furfural and 5-methyl furfural) are greatly increased by the catalysts employed. With regard to the selectivity, the  $\text{SO}_4^{2-}/\text{TiO}_2$  was reported to favor the formation of furfural and the  $\text{SO}_4^{2-}/\text{ZrO}_2$  favored the formation of furan, while the  $\text{SO}_4^{2-}/\text{SnO}_2$  was the most effective catalyst for obtaining 5-methyl furfural. The catalyst quantity was varied from 0.5 to 2 mg, of  $\text{SO}_4^{2-}/\text{SnO}_2$  catalyst at 500 °C, and it was reported that the yield of 5-methyl furfural was increased by 70–90 times (Lu et al., 2009).

### 3.17. Mesostructured sulfated tin oxide and its high catalytic activity in esterification and Friedel–Crafts acylation

Du et al. prepared a mesostructured sulfated tin oxide catalyst (MST) possessing large surface area ( $172 \text{ m}^2/\text{g}$ ) while employing block copolymer as template, followed by the sulfation of the sample. These catalysts were employed in the esterification reactions and Friedel–Crafts acylation reactions and it was found that it is more effective methodology than the conven-

**Table 11** Catalytic benzylation of toluene with benzoyl chloride over various samples (Du et al., 2006).

| Catalyst | Yield (%) | Selectivity |      |      |
|----------|-----------|-------------|------|------|
|          |           | Ortho       | Meta | Para |
| MST-500  | 89.2      | 20.0        | 3.7  | 77.3 |
| CST-500  | 81.0      | 23.0        | 3.5  | 73.5 |
| MST-550  | 79.8      | 19.6        | 3.5  | 76.9 |
| CST-550  | 74.6      | 23.4        | 3.3  | 73.3 |

**Table 12** Textual properties of various samples (Du et al., 2006).

| Sample  | BET ( $\text{m}^2/\text{g}$ ) | Pore volume ( $\text{cm}^3/\text{g}$ ) | Pore size (nm) | Sulfate content (%) |
|---------|-------------------------------|--|----------------|---------------------|
| MST-500 | 172                           | 0.17                                   | 3.1            | 4.78                |
| MST-550 | 97                            | 0.12                                   | 3.9            | 3.48                |
| CST-500 | 93                            | 0.13                                   | –              | 3.31                |
| CST-550 | 72                            | 0.10                                   | –              | 2.96                |

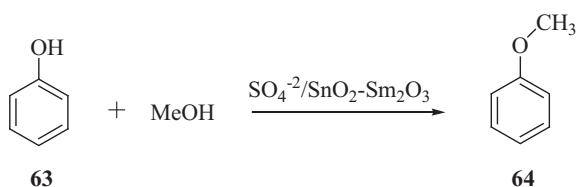
tional ones (Du et al., 2006). It was found that MST is more effective than the standard sulfated tin oxide. It was also observed that for the formation of strong acidic sites in sulfated tin oxide, the crystalline tetragonal phase  $\text{SnO}_2$  in MST is necessary.

Table 11 shows a comparative study of the catalytic activity of MST-X (where X stands for calcination temperature) and CST-X (conventional sulfated tin oxide) in Friedel–Crafts acylation of toluene with benzoyl chloride carried out at 100 °C. Table 12 shows a comparative study of the sulfate content, volume, and size of the MST-X and CST-X samples. The higher catalytic activity of the MST-X sample is mainly attributed to these values.

### 3.18. Alkylation of phenol with methanol

Jyothi et al. reported a comparative study of the tin-samarium binary oxide and its sulfate modified analogue ( $\text{SO}_4^{2-}/\text{SnO}_2\text{–Sm}_2\text{O}_3$ ) in the alkylation of phenol with methanol (Jyothi et al., 2000a,b,c). In the alkylation of phenol, the reaction pathway and the product selectivity are altered by the sulfate content. This is ascribed to the creation of strong acid sites on sulfation that enhances the adsorption of phenol on the catalyst surface as demonstrated in Scheme 19.

The physicochemical characteristics of the various oxides are as shown in Table 13. By the sulfate treatment, the super acid



**Scheme 19** Rare earth promoted STO-Catalyzed alkylation of phenol.

**Table 13** Physicochemical characteristics of oxides (Jyothi et al., 2000a,b,c).

| Catalyst                       | Surface area (m <sup>2</sup> /g) | Pore volume (cm <sup>3</sup> /g) | Average particle size (nm) | SO <sub>3</sub> (%) | Acid strength            |
|--------------------------------|----------------------------------|----------------------------------|----------------------------|---------------------|--------------------------|
| SnO <sub>2</sub>               | 36.1                             | 0.45                             | 9.70                       | –                   | –                        |
| TS82                           | 102.7                            | 0.31                             | 2.55                       | –                   | –                        |
| STS82                          | 190.8                            | 0.27                             | 2.12                       | 4.8                 | pK <sub>a</sub> ≤ –13.75 |
| Sm <sub>2</sub> O <sub>3</sub> | 28.2                             | 0.39                             | 7.60                       | –                   | –                        |

TS82: SnO<sub>2</sub> (80%)–Sm<sub>2</sub>O<sub>3</sub> (20%) binary mixed oxide; STS82: Sm-promoted sulfated SnO<sub>2</sub>.

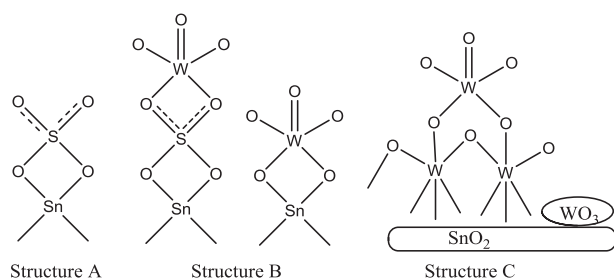
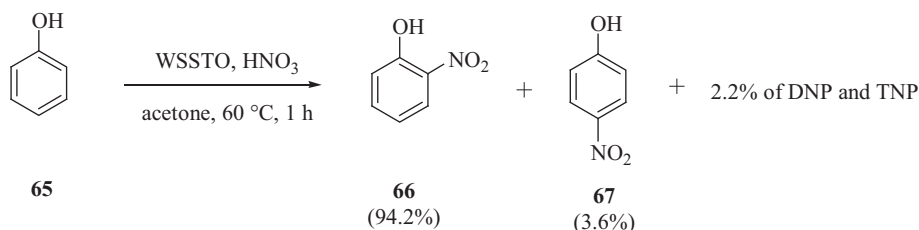


**Figure 24** Possible structures of the catalyst surface as a function of WO<sub>3</sub> loading. (Khder and Ahmed, 2009).

sites ( $H_0 \leq -13.75$ ) were created and the super acid character of the catalyst was retained even at high temperature (1073 K).

### 3.19. Selective nitration of phenol

WO<sub>3</sub> loaded nano-crystalline sulfated tin oxide solid acid catalyst was prepared and applied to analyze the selective nitration of the phenol. Based on the studies of the acidity measurements, the catalyst samples were shown to contain both the Lewis acid and Bronsted acid sites. It was found that with increase in the WO<sub>3</sub> content up to 30 wt% the acidity of



**Scheme 20** WO<sub>3</sub> loaded nano-crystalline STO catalyzed selective nitration of phenol.

the catalyst increased and it decreased with further increase in WO<sub>3</sub> content (Fig. 24). These results show the possibility of interaction of WO<sub>3</sub> with sulfate and SnO<sub>2</sub> surface. This interaction might have headed to changes in the surface structure of the catalyst. As demonstrated in Scheme 20, the catalytic activity was well correlated with the Bronsted acid sites (Khder and Ahmed, 2009).

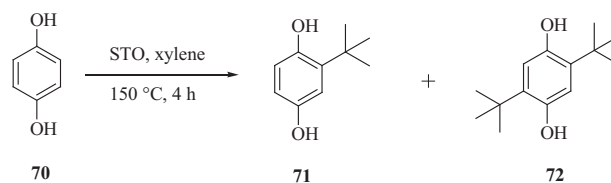
### 3.20. Alkylation of hydroquinone with *tert*-butanol

2-*tert*-Butylhydroquinone (2-TBHQ) is a renowned antioxidant in the food industry. It is also employed as an important precursor for the preparation of other chemicals as well as good stabilizer for plastics. This industrially important chemical is also prepared employing sulfated tin oxide as a catalyst, for the alkylation reaction of hydroquinone by *tert*-butanol and it was found to display high catalytic activity at 150 °C as illustrated in Scheme 21. A 96% conversion product 2-*tert*-butylhydroquinone was obtained at 150 °C (Zhou et al., 2008). One more observation reported was that during the reaction the catalyst was not deactivated in the first four runs. The high efficiency of the catalyst is because of the presence of the hydrophobic surface due to which the poisoning of the acid sites with water during the reaction was not feasible. It was also proposed that due to the weak acid sites, the possibility of formation of tar or polymeric compounds, usually formed by the side reactions on the surface is meager, due to which the reusability of the catalyst turns out to be high.

The results obtained indicated that the all sulfated tin oxide catalysts display elevated catalytic performance toward the alkylation reaction, which is found to be much higher than that of MCM-49, which is considered as an efficient catalyst for similar reaction. Table 14 and 15 reveal the activities of various sulfated metal oxides, for alkylation of hydroquinone, which were tested.

### 3.21. Direct oxidation of *n*-heptane to ester over modified sulfated SnO<sub>2</sub> catalysts under mild conditions

By employing the chemical co-precipitation method, the cobalt modified sulfated tin oxide (SO<sub>4</sub><sup>2-</sup>/SnO<sub>2</sub>–CO<sub>2</sub>O<sub>3</sub>) catalyst was



**Scheme 21** STO-Catalyzed alkylation of hydroquinone with *t*-butanol.

**Table 14** Activity of alkylation of hydroquinone over various sulfated tin oxide catalysts (Zhou et al., 2008).

| Catalyst  | T (°C) | Conversion (%) | Selectivity (%) |           |           | Yield (%) |
|---|--------|----------------|-----------------|-----------|-----------|-----------|
|   |        |                | 2-TBHQ          | 2,5-DTBHQ | 2,5-DTBHQ |           |
| SO <sub>4</sub> <sup>2-</sup> /SnO <sub>2</sub> (150) | 150    | 65             | 71              | 11        | 18        | 46        |
| SO <sub>4</sub> <sup>2-</sup> /SnO <sub>2</sub> (300) | 150    | 81             | 76              | 21        | 3         | 62        |
| SO <sub>4</sub> <sup>2-</sup> /SnO <sub>2</sub> (350) | 150    | 96             | 68              | 24        | 8         | 65        |
| SO <sub>4</sub> <sup>2-</sup> /SnO <sub>2</sub> (400) | 150    | 83             | 75              | 14        | 11        | 62        |
| SO <sub>4</sub> <sup>2-</sup> /SnO <sub>2</sub> (450) | 150    | 75             | 78              | 11        | 11        | 59        |
| SO <sub>4</sub> <sup>2-</sup> /SnO <sub>2</sub> (500) | 150    | 69             | 79              | 11        | 10        | 55        |
| SO <sub>4</sub> <sup>2-</sup> /SnO <sub>2</sub> (600) | 150    | 43             | 82              | 5         | 13        | 35        |
| SO <sub>4</sub> <sup>2-</sup> /SnO <sub>2</sub> (350) | 130    | 71             | 73              | 24        | 3         | 52        |
| SO <sub>4</sub> <sup>2-</sup> /SnO <sub>2</sub> (350) | 140    | 77             | 75              | 22        | 3         | 58        |
| MCM-49(20)  | 150    | 50             | 65              | 25        | 10        | 33        |

Reaction mixture: 0.5 g hydroquinone and 1.0 g *tert*-butanol in 2 g xylene; catalyst: 0.2; reaction condition: 130–150 °C for 4 h.

**Table 15** Activity of alkylation of hydroquinone over various sulfated metal oxides (Zhou et al., 2008).

| Catalyst  | Conversion (%) | Selectivity (%)     |                        |                   |                        | 2-TBHQ Yield (%) |
|---|----------------|---------------------|------------------------|-------------------|------------------------|------------------|
|   |                | 2-TBHQ <sup>a</sup> | 2,5-DTBHQ <sup>b</sup> | TBPE <sup>c</sup> | 2,5-DTBHQ <sup>d</sup> |                  |
| SO <sub>4</sub> <sup>2-</sup> /SnO <sub>2</sub>               | 96             | 68                  | 24                     | 0                 | 8                      | 65               |
| SO <sub>4</sub> <sup>2-</sup> /TiO <sub>2</sub>               | 98             | 49                  | 14                     | 0                 | 37                     | 48               |
| SO <sub>4</sub> <sup>2-</sup> /Fe <sub>2</sub> O <sub>3</sub> | 99             | 49                  | 27                     | 0                 | 24                     | 49               |
| SO <sub>4</sub> <sup>2-</sup> /Al <sub>2</sub> O <sub>3</sub> | 49             | 53                  | 18                     | 18                | 22                     | 26               |
| SO <sub>4</sub> <sup>2-</sup> /MgO                            | 25             | 3                   | 0                      | 93                | 4                      | 0.8              |
| SO <sub>4</sub> <sup>2-</sup> /CuO                            | 17             | 1                   | 0                      | 94                | 5                      | 0.2              |
| SO <sub>4</sub> <sup>2-</sup> /NiO                            | 12             | 0                   | 0                      | 97                | 3                      | 0                |
| SO <sub>4</sub> <sup>2-</sup> /MnO                            | 8.7            | 9                   | 0                      | 91                | 0                      | 0.8              |
| SO <sub>4</sub> <sup>2-</sup> /ZnO                            | 8.6            | 3                   | 0                      | 92                | 5                      | 0.3              |
| SO <sub>4</sub> <sup>2-</sup> /ZnO                            | 8.2            | 0                   | 0                      | 100               | 0                      | 0                |
| SO <sub>4</sub> <sup>2-</sup> /BaO                            | 1.8            | 12                  | 10                     | 78                | 0                      | 0.2              |

Reaction mixture: 0.5 g hydroquinone and 1.0 g *tert*-butanol in 2 g xylene; catalyst: 0.2; reaction condition: 150 °C for 4 h.

<sup>a</sup> Represents 2-*tert*-butyl hydroquinone.

<sup>b</sup> Represents 2,5-di-*tert*-butyl hydroquinone.

<sup>c</sup> Represents *tert*-butyl phenol ether (TBPE).

<sup>d</sup> Represents 2,5-di-*tert*-butyl benzoquinone (2,5-DTBBQ).

prepared along with the sulfated tin oxide (SO<sub>4</sub><sup>2-</sup>/SnO<sub>2</sub>) and these catalysts were characterized by the SEM, XRD, FT-IR and XPS techniques. Thus prepared catalysts were used in the direct oxidation of *n*-heptane to ester using air as the oxidant under the mild conditions (Cui et al., 2007). From the observations made by authors, the SO<sub>4</sub><sup>2-</sup>/SnO<sub>2</sub>–CO<sub>2</sub>O<sub>3</sub> is found to be best catalyst than SO<sub>4</sub><sup>2-</sup>/SnO<sub>2</sub> in the oxidation of *n*-pentane. Asymmetric esters such as diisobutyl phthalate and cyclohexylmethyl tridecyl oxalate have been synthesized from this method whereas all other conventional methods failed.

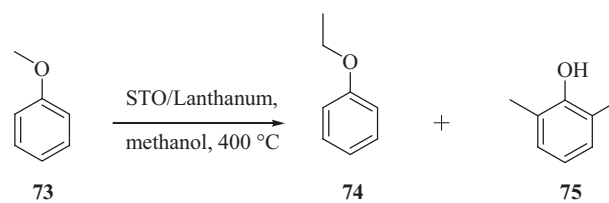
### 3.22. Dealkylation of anisole to phenol using lanthanum-sulfated SnO<sub>2</sub>

In the year 2000, a comparative study on the lanthanum-promoted SnO<sub>2</sub> catalyst and its sulfate-doped analogue for the methylation of anisole with methanol was reported by Jyothi et al. (2000a,b,c). A maximum selectivity of 82% (for 75) was obtained under the optimized reaction conditions, at 400 °C. This is found to be formed by isomerization of methyl anisole over lanthanum-promoted SnO<sub>2</sub> catalyst and mainly

because of the presence of weak Lewis acid sites and comparatively stronger basic sites. As shown in Scheme 22, the sulfate modification resulted in the dealkylation of anisole and several unwanted side reactions (due to the creation of strong acidic sites).

### 3.23. Olefin polymerization and hydrogenation catalysis

Sulfated tin oxide particles of ~5 nm size were prepared and they are used as effective supporters in the homogeneous zirconium hydrocarbyl olefin polymerization and arene hydrogenation.



**Scheme 22** Lanthanum-sulfated SnO<sub>2</sub> catalyzed dealkylation of anisole.

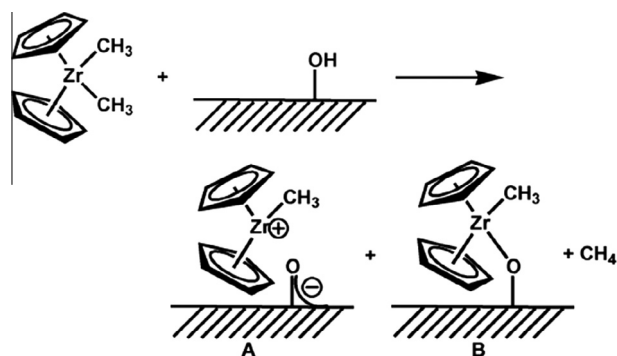
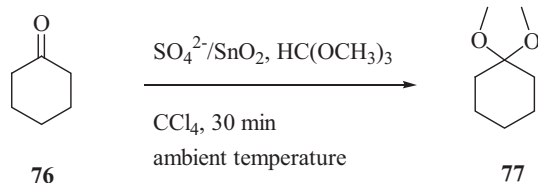
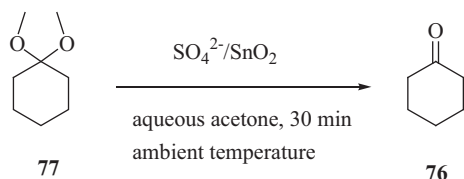


**Figure 25** STO nanoparticles for olefin polymerization and arene hydrogenation (Nicholas and Marks, 2004).



**Scheme 23** Mesoporous STO-Catalyzed synthesis of dimethyl acetals.



**Scheme 24** Mesoporous STO-Catalyzed deprotection of dimethyl acetals.

tion catalysis (Nicholas and Marks, 2004). Nicholas et al. demonstrated that the group hydrocarbonyl chemisorption on “super” Bronsted acidic sulfated metal oxide (SMO) surfaces produces a highly lively catalysts, which possess 100% active sites that can be employed for the polymerization of olefins and hydrogenation of arene (Fig. 25) (Nicholas et al., 2003). Here, the SMO converts the neutral organometallic precursor into a catalytically-active electrophile, which makes it eco-catalyst/activator, and also a support, stabilizing the bound molecular adsorbate.

### 3.24. Synthesis and hydrolysis of dimethyl acetals

The mesoporous sulfated tin oxide was found to be an efficient catalyst for the synthesis of dimethyl acetals by the reaction between aldehydes/ketones and trimethyl orthoformate under milder reaction conditions (Lin et al., 2001). As illustrated in Scheme 23, the corresponding dimethyl acetals were produced from the carbonyl compounds in 83–100% yield at room temperature.

It is observed that the mesoporous sulfated tin oxide catalyzes the hydrolysis of dimethyl acetal to regenerate the original carbonyl compound. The solvent employed for this reaction is aqueous acetone (Scheme 24). Hence, this synthetic

protocol is not only effective for the synthesis of dimethyl acetals of larger molecular weight but also an effective method for protection and deprotection of carbonyl groups in synthetic organic chemistry.

### 3.25. Ethanol oxidation

Zhang et al. reported the preparation of the Pt–S–SnO<sub>2</sub>/MWCNTs catalyst by a blending the sol–gel method, with pulse-microwave assisted polyol method. The obtained catalyst was tested as oxidation catalyst for ethanol oxidation, and the results indicate that the catalyst exhibits superior catalytic activity than the non-sulfated Pt supported on SnO<sub>2</sub>/MWCNTs composites due to increased proton conductivity of sulfated SnO<sub>2</sub> (Scott et al., 2003; Zhang et al., 2011).

### 3.26. Catalysis in direct coal liquefaction

Highly dispersed forms of certain metal catalysts found to be very active for the conversion of coal to liquid (coal liquefaction) (Suzuki et al., 1989). The tin oxide on sulfation, reduces the average particle diameter and increases the specific surface area available for catalysis and hence increases the dispersion of the catalyst (Pradhan et al., 1991). So, the sulfated tin oxide solid acid catalyst was found to be useful for the direct liquefaction of the coal. The sulfate group was also found to increase the acidity of the catalysts (from the data obtained from FT-IR and pyridine adsorption). The sulfated tin oxide catalyst was found to be a better hydrogenolysis catalyst for the hydrodesulfurization and hydro-denitrogenation reactions.

## 4. Conclusion

Sulfated metal oxides (SMOs) including ZrO<sub>2</sub>, SnO<sub>2</sub>, TiO<sub>2</sub> and Fe<sub>2</sub>O<sub>3</sub> possess both Bronsted acid sites derived from sulfates fixed on the surface of metal oxides and Lewis acid sites derived from metal oxides, due to which they have been widely used as a solid-acid catalyst in a variety of organic transformations. These low cost catalysts are eco-friendly, non-corrosive and possess greater stability, displaying high efficiency toward catalytic performance. They can also be easily recovered from the reaction mixture by simple filtration and re-used after activation. Among the many that are reported in the literature, sulfated tin oxide (SO<sub>4</sub><sup>2-</sup>/SnO<sub>2</sub>) catalyst has been extensively used in various organic transformations such as hydrocracking of paraffins, dehydration of alcohols, esterification, alkylation of olefins, photochemical catalysis and protection of aldehydes, ketones and alcohols and olefin. In this review, we have covered characterization and applications of STO, which can be useful for the researchers dealing with tin catalyzed reactions. The nature of their super acidity, heterogeneity, the identities of the active sites and their use in various synthetic transformation reactions have highlighted that this catalyst can be further exploited for various other transformations. From the above literature reports it can be concluded that sulfated tin oxide (II) is far better than its unsulfated precursor in display of catalytic performance, which is attributed to the generation of Bronsted-lewis acid sites in the catalyst. The same can be attempted in various other metal oxide salts and can be tested for different organic transformations which can be taken up as a future study.

## Acknowledgments

This project was supported by King Saud University, Deanship of Scientific Research, College of Science, Research Centre. Dr. Ravi Varala thanks Prof. Appala Naidu, Registrar,

RGUKT, Prof. S. Satyanarayana, VC-RGUKT, Prof. Zubaidha Pudukulathan (SRTMU, Nanded), Prof. Osvaldo Novais Oliveira Jr., IFSC-USP, Brazil, for their encouragement and support.

## References

- Ahmed, A.I., El-Hakam, S., et al, 2013. Nanostructure sulfated tin oxide as an efficient catalyst for the preparation of 7-hydroxy-4-methyl coumarin by Pechmann condensation reaction. *J. Mol. Catal. A: Chem.* 366, 99–108.
- Alam, M.M., Merajuddin, A.S., et al, 2014. An efficient solvent free one-pot synthesis of naphtha pyranopyrimidines under microwave irradiation catalyzed by sulfated tin oxide. *Int. J. Basic Appl. Chem. Sci.* 4, 24–29.
- Arata, K., 1990. Solid superacids. *Adv. Catal* 37, 165.
- Arata, K., 1996. Preparation of superacids by metal oxides for reactions of butanes and pentanes. *Appl. Catal. A* 146, 3–32.
- Arata, K., 2009. Organic syntheses catalyzed by superacidic metal oxides: sulfated zirconia and related compounds. *Green Chem.* 11, 1719–1728.
- Arata, K., Matsuhashi, H., et al, 2003. Synthesis of solid superacids and their activities for reactions of alkanes. *Catal. Today* 81, 17–30.
- Arena, F., Deiana, C., et al, 2015. Activity patterns of metal oxide catalysts in the synthesis of *N*-phenylpropionamide from propanoic acid and aniline. *Catal. Sci. Tech.* 5, 1911–1918.
- Batzill, M., Diebold, U., 2005. The surface and materials science of tin oxide. *Prog. Surf. Sci.* 79, 47–154.
- Bhure, M.H., Kumar, I., et al, 2008. Facile and highly selective deprotection of tert-butyl dimethyl silyl ethers using sulfated SnO<sub>2</sub> as a solid catalyst. *Syn. Commun.* 38, 346–353.
- Brown, A.C., Hargreaves, J.J., 1999. Sulfated metal oxide catalysts. Superactivity through superacidity? *Green Chem.* 1, 17–20.
- Célérier, S., Richard, F., 2015. Promising heterogeneous catalytic systems based on metal fluorides and oxide hydroxide fluorides: a short review. *Catal. Commun.* 67, 26–30.
- Chavan, S.P., Zubaidha, P., et al, 1996. Use of solid superacid (sulphated SnO<sub>2</sub>) as efficient catalyst in facile transesterification of ketoesters. *Tetrahedron Lett.* 37, 233–236.
- Clearfield, A., Serrette, G., et al, 1994. Nature of hydrous zirconia and sulfated hydrous zirconia. *Catal. Today* 20, 295–312.
- Connell, G., Dumesic, J., 1986. Acidic properties of binary oxide catalysts: II. Mössbauer spectroscopy and pyridine adsorption for iron supported on magnesia, alumina, and titania. *J. Catal.* 102, 216–233.
- Corma, A., Iborra, S., et al, 2007. Chemical routes for the transformation of biomass into chemicals. *Chem. Rev.* 107, 2411–2502.
- Cui, X., Ma, H., et al, 2007. Direct oxidation of *n*-heptane to ester over modified sulfated SnO<sub>2</sub> catalysts under mild conditions. *J. Hazard. Mater.* 147, 800–805.
- Dabbawala, A.A., Mishra, D.K., et al, 2013. Sulfated tin oxide as an efficient solid acid catalyst for liquid phase selective dehydration of sorbitol to isosorbide. *Catal. Commun.* 42, 1–5.
- Dake, S.A., Khedkar, M.B., et al, 2012. Sulfated tin oxide: a reusable and highly efficient heterogeneous catalyst for the synthesis of 2, 4, 5-triaryl-1H-imidazole derivatives. *Syn. Commun.* 42, 1509–1520.
- Du, Y., Liu, S., et al, 2008. Synthesis of sulfated silica-doped tin oxides and their high activities in transesterification. *Catal. Lett.* 124, 133–138.
- Du, Y., Liu, S., et al, 2006. Mesoporous sulfated tin oxide and its high catalytic activity in esterification and Friedel–Crafts acylation. *Catal. Lett.* 108, 155–158.
- El-Sharkawy, E., Al-Shihry, S.S., 2010. Friedel–Crafts acylation of toluene using superacid catalysts in a solvent-free medium. *Monatsh. Chem.* 141, 259–267.
- Furuta, S., Matsuhashi, H., et al, 2004a. Biodiesel fuel production with solid superacid catalysis in fixed bed reactor under atmospheric pressure. *Catal. Commun.* 5, 721–723.
- Furuta, S., Matsuhashi, H., et al, 2004b. Catalytic action of sulfated tin oxide for etherification and esterification in comparison with sulfated zirconia. *Appl. Catal. A* 269, 187–191.
- Gawande, M.B., Pandey, R.K., et al, 2012. Role of mixed metal oxides in catalysis science – versatile applications in organic synthesis. *Catal. Sci. Tech.* 2, 1113–1125.
- Gilbert, J.C., Kelly, T.A., 1988. Transesterification of 3-oxo esters with allylic alcohols. *J. Org. Chem.* 53, 449–450.
- Greenwood, N.N., Earnshaw, A., 1984. Chemistry of the elements. *Angew. Chem. Int. Ed.* 97, 719–720.
- Guo, H.-F., Yan, P., et al, 2008. Influences of introducing Al on the solid super acid SO<sub>4</sub><sup>2-</sup>/SnO<sub>2</sub>. *Mater. Chem. Phys.* 112, 1065–1068.
- Hudlicky, T., Claeboe, C.D., et al, 1999. Use of electrochemical methods as an alternative to tin reagents for the reduction of vinyl halides in inositol synthons. *J. Org. Chem.* 64, 4909–4913.
- Jensen, W.B., 2002. Holleman–Wiberg’s inorganic chemistry (edited by Wiberg, Nils). *J. Chem. Educ.* 79, 944.
- Jogalekar, A., Jaiswal, R., et al, 1998. Activity of modified SnO<sub>2</sub> catalysts for acid-catalysed reactions. *J. Chem. Technol. Biotechnol.* 71, 234–240.
- José da Silva, M., Lemos Cardoso, A., 2013. Heterogeneous tin catalysts applied to the esterification and transesterification reactions. *J. Catal.*
- Jyothi, T., Sreekumar, K., et al, 2000a. Alkylation of phenol with methanol over rare earth promoted sulfated tin oxide catalyst. *React. Kinet. Catal. Lett.* 69, 339–343.
- Jyothi, T., Sreekumar, K., et al, 2000b. Physico-chemical characteristic of sulfated mixed oxides of Sn with some rare earth elements. *Pol. J. Chem.* 74, 801–812.
- Jyothi, T., Sugunan, S., et al, 2000c. A comparative study on the anisole methylation activity of lanthanum-promoted SnO<sub>2</sub> catalyst and its sulfate-doped analogue. *Catal. Lett.* 70, 187–190.
- Kafuku, G., Lam, M.K., et al, 2010a. *Croton megalocarpus* oil: a feasible non-edible oil source for biodiesel production. *Bioresour. Technol.* 101, 7000–7004.
- Kafuku, G., Lee, K., et al, 2010b. The use of sulfated tin oxide as solid superacid catalyst for heterogeneous transesterification of *Jatropha curcas* oil. *Chem. Pap.* 64, 734–740.
- Kafuku, G., Mbarawa, M., 2010. Alkaline catalyzed biodiesel production from *Moringa oleifera* oil with optimized production parameters. *Appl. Energy* 87, 2561–2565.
- Khalaf, H.A., Mansour, S.E., et al, 2011. The influence of sulfate contents on the surface properties of sulfate-modified tin(IV) oxide catalysts. *J. Assoc. Arab Un. Basic App. Sci.* 10, 15–20.
- Khder, A., Ahmed, A., 2009. Selective nitration of phenol over nanosized tungsten oxide supported on sulfated SnO<sub>2</sub> as a solid acid catalyst. *Appl. Catal. A* 354, 153–160.
- Khder, A., El-Sharkawy, E., et al, 2008. Surface characterization and catalytic activity of sulfated tin oxide catalyst. *Catal. Commun.* 9, 769–777.
- Kiss, A.A., Dimian, A.C., et al, 2007. Biodiesel by catalytic reactive distillation powered by metal oxides. *Energy Fuels* 22, 598–604.
- Lam, M.K., Lee, K.T., 2010. Accelerating transesterification reaction with biodiesel as co-solvent: a case study for solid acid sulfated tin oxide catalyst. *Fuel* 89, 3866–3870.
- Lam, M.K., Lee, K.T., Mohamed, A.R., 2009. Sulfated tin oxide as solid superacid catalyst for transesterification of waste cooking oil: an optimization study. *Appl. Catal. B* 93 (1–2), 134–139.
- Lin, C.-H., Lin, S.D., et al, 2001. The synthesis and hydrolysis of dimethyl acetals catalyzed by sulfated metal oxides. An efficient method for protecting carbonyl groups. *Catal. Lett.* 73, 121–125.
- Lotero, E., Liu, Y., et al, 2005. Synthesis of biodiesel via acid catalysis. *Ind. Eng. Chem. Res.* 44, 5353–5363.

- Lu, Q., Xiong, W.-M., et al, 2009. Catalytic pyrolysis of cellulose with sulfated metal oxides: a promising method for obtaining high yield of light furan compounds. *Bioresour. Technol.* 100, 4871–4876.
- Magar, R.L., Thorat, P.B., et al, 2013. Distereoselective one-pot synthesis of pyrimidopyrimidines using sulfated tin oxide as a reusable catalyst: an extension of Biginelli-type reaction. *Chin. Chem. Lett.* 24, 1070–1074.
- Matsuhashi, H., Miyazaki, H., et al, 2001a. The preparation of solid superacid of sulfated tin oxide with acidity higher than sulfated zirconia. *Chem. Lett.*, 452–453
- Matsuhashi, H., Miyazaki, H., et al, 2001b. Preparation of a solid superacid of sulfated tin oxide with acidity higher than that of sulfated zirconia and its applications to aldol condensation and benzoylation. *Chem. Mater.* 13, 3038–3042.
- Mekhemer, G.A., 2006. Surface characterization of zirconia, holmium oxide/zirconia and sulfated zirconia catalysts. *Colloids Surf. A* 274, 211–218.
- Mekhemer, G.A., Khalaf, H.A., et al, 2005. Sulfated alumina catalysts: consequences of sulfate content and source. *Monatsh. Chem.* 136, 2007–2016.
- Moreno, J., Jaimes, R., et al, 2011. Evaluation of sulfated tin oxides in the esterification reaction of free fatty acids. *Catal. Today* 172, 34–40.
- Naik, M.A., Mishra, B.G., et al, 2009. Catalytic applications of sulfated tin oxide for synthesis of structurally diverse  $\beta$ -acetamido ketones and aryl-14*H*-dibenzo [a] xanthenes. *Bull. Catal. Soc. India* 8, 35–40.
- Nakamoto, K., 1986. *Infrared and Raman Spectra of Inorganic and Coordination Compounds: Part A: Theory and Applications in Inorganic Chemistry*, sixth ed. John Wiley & Sons, Inc.
- Narayana, V., Varala, R., et al, 2012.  $\text{SO}_4^{2-}/\text{SnO}_2$ -catalyzed C3-alkylation of 4-hydroxycoumarin with secondary benzyl alcohols and *O*-alkylation with *O*-acetyl compounds. *Int. J. Org. Chem.* 2, 287–294.
- Narayana, V.R., Pudukulathan, Z., et al, 2013.  $\text{SO}_4^{2-}/\text{SnO}_2$ -catalyzed efficient one-pot synthesis of 7, 8-dihydro-2*H*-chromen-5-ones by formal [3+ 3] cycloaddition and 1, 8-dioxo-octahydroxanthenes via a Knoevenagel condensation. *Org. Commun.* 6, 110–119.
- Nicholas, C.P., Ahn, H., et al, 2003. Synthesis, spectroscopy, and catalytic properties of cationic organozirconium adsorbates on “super acidic” sulfated alumina. “Single-site” heterogeneous catalysts with virtually 100 active sites. *J. Am. Chem. Soc.* 125, 4325–4331.
- Nicholas, C.P., Marks, T.J., 2004. Sulfated tin oxide nanoparticles as supports for molecule-based olefin polymerization catalysts. *Nano Lett.* 4, 1557–1559.
- Norman, C., Goulding, P., et al, 1994. 3.4 The role of sulphate in the stabilisation of zirconia. *Stud. Surf. Sci. Catal.* 90, 269–272.
- Nuithitikul, K., Prasitturattanachai, W., et al, 2011. Catalytic activity of sulfated iron–tin mixed oxide for esterification of free fatty acids in crude palm oil: effects of iron precursor, calcination temperature and sulfate concentration. *Int. J. Chem. React. Eng.* 9.
- Park, J.Y., Baker, L.R., et al, 2015. Role of hot electrons and metal–oxide interfaces in surface chemistry and catalytic reactions. *Chem. Rev.* 115, 2781–2817.
- Pradhan, V.R., Tierney, J.W., et al, 1991. Catalysis in direct coal liquefaction by sulfated metal oxides. *Energy Fuels* 5, 497–507.
- Prasitturattanachai, W., Nuithitikul, K., 2013. Esterification of free fatty acids in crude palm oil using alumina-doped sulfated tin oxide as a catalyst. In: *Proceedings of World Academy of Science, Engineering and Technology, World Academy of Science, Engineering and Technology (WASET)*, vol. 79, p. 821.
- Radi, M., Schenone, S., et al, 2009. Recent highlights in the synthesis of highly functionalized pyrimidines. *Org. Biomol. Chem.* 7, 2841–2847.
- Ren, Y., Ma, Z., et al, 2012. Ordered mesoporous metal oxides: synthesis and applications. *Chem. Soc. Rev.* 41, 4909–4927.
- Sarda, S.R., Puri, V.A., et al, 2007. Sulfated tin oxides: a suitable reagent for synthesis of 2, 4-diphenyl-4, 6, 7, 8-tetrahydrochromen-5-one. *Arkivoc* 16, 246–251.
- Scott, R.W., Mamak, M., et al, 2003. Making sense out of sulfated tin dioxide mesostructures. *J. Mater. Chem.* 13, 1406–1412.
- Searle, A.B., 2008. *The Glazer’s Book – The Practical Application of Recipes and Processes to Glazes for Bricks and Tiles*. Wright Press.
- Sheldon, R., 1993. The role of catalysis in waste minimization. In: *Precision Process Technology*. Springer, pp. 125–138.
- Sheldon, R.A., 2000. Atom efficiency and catalysis in organic synthesis. *Pure Appl. Chem.* 72, 1233–1246.
- Suzuki, T., Yamada, H., et al, 1989. Hydrogenation and hydrogenolysis of coal model compounds by using finely dispersed catalysts. *Energy Fuels* 3, 707–713.
- Suzuki, T., Yokoi, T., et al, 2011. Dehydration of xylose over sulfated tin oxide catalyst: influences of the preparation conditions on the structural properties and catalytic performance. *Appl. Catal. A* 408, 117–124.
- Waqif, M., Bachelier, J., et al, 1992. Acidic properties and stability of sulfate-promoted metal oxides. *J. Mol. Catal.* 72, 127–138.
- Watson, J., 1984. The tin oxide gas sensor and its applications. *Sens. Actuat. A* 5, 29–42.
- Wiglenda, T., Ott, I., et al, 2005. Synthesis and pharmacological evaluation of 1*H*-imidazoles as ligands for the estrogen receptor and cytotoxic inhibitors of the cyclooxygenase. *J. Med. Chem.* 48, 6516–6521.
- Yang, Z.-W., Chen, L.-N., et al, 2012. Baeyer–Villiger oxidation and acetalization of cyclic ketones on  $\text{SO}_4^{2-}/\text{SnO}_2\text{-Fe}_2\text{O}_3$  solid acid catalysts. *Acta Phys.-Chim. Sin.* 28, 2148–2154.
- Yu, H., Fang, H., et al, 2009. Acidity of sulfated tin oxide and sulfated zirconia: a view from solid-state NMR spectroscopy. *Catal. Commun.* 10, 920–924.
- Zhai, D.-W., Yue, Y.-H., et al, 2010. Esterification and transesterification on  $\text{Al}_2\text{O}_3$ -doped sulfated tin oxide solid acid catalysts. *Acta Phys.-Chim. Sin.* 26, 1867–1872.
- Zhai, D., Nie, Y., et al, 2011. Esterification and transesterification on  $\text{Fe}_2\text{O}_3$ -doped sulfated tin oxide catalysts. *Catal. Commun.* 12, 593–596.
- Zhang, X., Zhu, H., et al, 2011. Sulfated  $\text{SnO}_2$  modified multi-walled carbon nanotubes – a mixed proton–electron conducting support for Pt catalysts in direct ethanol fuel cells. *J. Power Sources* 196, 3048–3053.
- Zhou, L., Xu, B., et al, 2008. Sulfated tin oxide: an efficient catalyst for alkylation of hydroquinone with *tert*-butanol. *Catal. Commun.* 9, 2274–2277.
- 倉員貴昭, 2011. The second international conference on bioenvironment, biodiversity and renewable energies, BIONATURE 2011 国際会議参加報告. *日本水産学会誌* 77, 944.